

"The Handbook of Environmental Chemistry Series"
Vol. 5: Water Pollution, Part H (Estuaries)
2006; VOL 5 265-301
http://dx.doi.org/10.1007/698_5_024
©XXX Springer Science+Business Media

Archimer, archive institutionnelle de l'Ifremer
<http://www.ifremer.fr/docelec/>

The original publication is available at <http://www.springerlink.com>

Role of Particle Sorption Properties in the Behavior and Speciation of Trace Metals in Macrotidal Estuaries: The Cadmium Example

J-L. Gonzalez^{1(*)}, B. Thouvenin¹, C. Dange¹, J-F. Chiffolleau² and B. Boutier²

¹Biogéochimie and Ecotoxicologie Department, IFREMER, Z.P. de Brégaillon, B.P. 330, 83507 La Seyne sur Mer, France

²Biogéochimie and Ecotoxicologie Department, IFREMER, Rue de l'Île d'Yeu, B.P. 21105, B.P. 21105, 44311 Nantes, France

*: Corresponding author : gonzalez@ifremer.fr

Abstract:

The role of particles in the fate and speciation of trace metals in macrotidal estuaries was studied using a surface complexation model (MOCO). Cadmium was selected as the target metal contaminant due to its reactivity in estuaries: cadmium behavior is mainly controlled by heterogeneous processes (sorption/desorption) related to salinity and suspended matter gradients.

Various scenarios of suspended matter distribution according to salinity were simulated. The impact of surface properties (specific surface area, density of surface sites, acido-basic properties, and complexation constant) was evaluated using data collected on particles from the Gironde, Loire, and Seine estuaries.

Our results show that particle surface properties, evaluated on the basis of various parameters, are instrumental in "non-conservative" contaminant speciation in the estuarine environment. Their evaluation enables us to understand and simulate, to a large extent, the fate of "Cd-type" contaminants (whose behavior is controlled by competition between sorption and desorption processes). The natural variations of these properties can be responsible for significant modifications of the Cd speciation in the macrotidal estuaries where salinity and SM gradients are very strong.

Keywords: Cadmium - Macrotidal estuaries - Modeling - Particles - Sorption - Speciation - Turbidity maximum

Role of Particle Sorption Properties in the Behavior and Speciation of Trace Metals in Macrotidal Estuaries: The Cadmium Example

J.-L. Gonzalez¹ (✉) · B. Thouvenin¹ · C. Dange¹ · J.-F. Chiffolleau² · B. Boutier²

¹Biogéochimie and Ecotoxicologie Department, IFREMER, Z.P. de Brégaillon, B.P. 330, 83507 La Seyne sur Mer, France
gonzalez@ifremer.fr

²Biogéochimie and Ecotoxicologie Department, IFREMER, Rue de l'Île d'Yeu, B.P. 21105, B.P. 21105, 44311 Nantes, France

| | | |
|-----|---|----|
| 1 | Introduction | 2 |
| 2 | Seine, Loire, and Gironde Estuaries: Main Characteristics | 5 |
| 3 | Particle Geochemical Characteristics and Surface Properties | 7 |
| 4 | Behavior of Cd in Macrotidal Estuaries | 10 |
| 5 | Presentation of the Model and Simulation Conditions | 16 |
| 6 | Results and Discussion | 20 |
| 6.1 | Global Sorption Capacity of Particles (GSC) | 20 |
| 6.2 | Simulation of Migration of the Turbidity Maximum | 22 |
| 6.3 | Simulation of the Presence of a Second Turbidity Maximum | 29 |
| 6.4 | Simulation of Turbidity Peaks | 31 |
| 7 | Summary and Conclusions | 31 |
| | References | 35 |

Abstract The role of particles in the fate and speciation of trace metals in macrotidal estuaries was studied using a surface complexation model (MOCO). Cadmium was selected as the target metal contaminant due to its reactivity in estuaries: cadmium behavior is mainly controlled by heterogeneous processes (sorption/desorption) related to salinity and suspended matter gradients.

Various scenarios of suspended matter distribution according to salinity were simulated. The impact of surface properties (specific surface area, density of surface sites, acido-basic properties, and complexation constant) was evaluated using data collected on particles from the Gironde, Loire, and Seine estuaries.

Our results show that particle surface properties, evaluated on the basis of various parameters, are instrumental in “non-conservative” contaminant speciation in the estuarine environment. Their evaluation enables us to understand and simulate, to a large extent, the fate of “Cd-type” contaminants (whose behavior is controlled by competition between sorption and desorption processes). The natural variations of these properties can be responsible for significant modifications of the Cd speciation in the macrotidal estuaries where salinity and SM gradients are very strong.

Keywords Cadmium · Macrotidal estuaries · Modeling · Particles · Sorption · Speciation · Turbidity maximum

Abbreviations

| | |
|----------------------------|--|
| ABT | Potentiometric acid-base titration |
| BET | Brunauer, Emmett, Teller |
| %CdD | Percentage of dissolved Cd |
| CEC | Cation exchange capacity in mol g^{-1} of SM |
| GSC | Global sorption capacity of particles |
| K | Complexation constant |
| K_{a1} and K_{a2} | Intrinsic surface acid-base constants of active surface sites |
| K_d | Partition coefficient |
| K_m | Global intrinsic complexation constant |
| POC | Particulate organic carbon |
| RSD | Relative standard deviation |
| SA | Specific particle surface area in $\text{m}^2 \text{g}^{-1}$ |
| SM | Suspended matter |
| $-\text{SOH}_{\text{tot}}$ | Total density of active surface sites in mol g^{-1} of SM |

1

Introduction

Estuaries are transition zones between continental hydrographic networks and the marine environment. These essential interfaces come in a vast number of shapes and sizes, and can be classified according to their degree of fresh-salt water mixing (well mixed: fjords; moderately stratified: macrotidal estuaries; highly stratified: deltas or microtidal estuaries). The estuary type is primarily defined by the balance of power between the upstream river (river flow) and the downstream ocean (spring tidal range) [1–3].^{TS^a}

Climatic and geological factors are also responsible for wide estuary variations. Each estuary has its own hydrologic and morphologic characteristics, meaning that, biologically speaking, specific communities can exist within each environment.

Due to their particular location and characteristics, these environments are often highly sought after as residential areas, fishing zones, or for the development of port installations and industrial activities. The Escaut and Seine estuaries constitute good examples of this on a European level: they both feature dense populations and rank among Europe's biggest industrial centers. They are also Europe's most highly contaminated estuaries. Anthropogenic activities all have a potentially significant and short-term impact on ecosystem structure and functioning, leading to the weakening, and possible eventual death, of the traditional economic interests associated with these environments.

^{TS^a} Please confirm short title

Just 5% of the estuaries located along the French coast spanning the English Channel and Atlantic are actually the mouths of major rivers, i.e., with mean water flows exceeding $50 \text{ m}^3 \text{ s}^{-1} \text{ year}^{-1}$ [4]. The Seine, Loire, and Gironde are ranked as France's three largest estuaries (Fig. 1), with mean annual flows of over $400 \text{ m}^3 \text{ s}^{-1}$.

The peculiar character of these macrotidal estuaries is forged by a large input of particles from their upstream rivers, coupled with a tidal amplitude $> 4 \text{ m}$ along the adjacent coasts, resulting in a high-impact dynamic tide (up to 150 km upstream of the mouth in the case of the Seine), the presence of a turbidity maximum, and extensive mud deposit zones.

The contaminant content of estuarine particles is not only the result of pollutant inputs; it may also be significantly modified and regulated by reactions occurring on the surface of particles (sorption/desorption), which also play a significant role in speciation and contaminant bioavailability.

Contaminants may be present in the aquatic environment in dissolved, colloidal, or particulate form. The distinction between these three forms is fixed arbitrarily by filtration (and ultrafiltration) according to size [5]. Within these operationally defined "physical" categories, contaminants may belong to various "chemical" species, according to their nature and type of association.

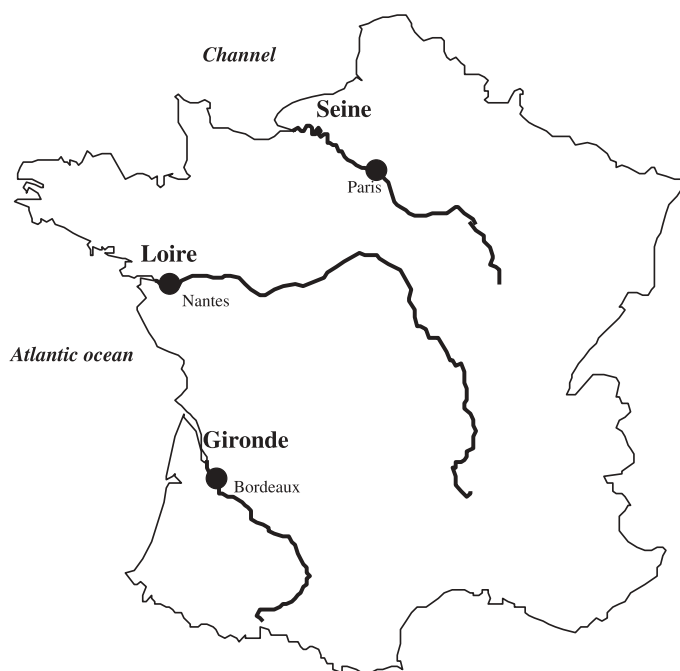


Fig. 1 Location of the Seine, Loire, and Gironde estuaries

Contaminant transition from one of these chemical species to another is controlled by various physicochemical and biological factors, including pH, redox potential, salinity, water concentrations of various complexation agents, sedimentologic characteristics, and particle geochemistry. The role of particles is particularly important in macrotidal estuaries, which are often characterized by the presence of a turbidity maximum [6]. Intra- and interestuary concentrations of suspended matter (SM) also vary widely (from a few milligrams to several grams per liter), according to river flow and tidal conditions. The repercussions of SM on biogeochemical cycles in the estuarine environment has already been underlined by Turner and Millward [7], along with the impact of salinity and particles on trace metal particulate-dissolved phase distribution [8].

Contaminant behavior during estuarine transit can be globally described as conservative (meaning the element stays in the same phase throughout estuary crossing) or non-conservative (meaning the element undergoes a process which modifies its distribution).

Cadmium is an excellent example of non-conservative behavior, and one of the most reactive metal contaminants found in the estuarine environment.

If the longitudinal evolution of dissolved Cd concentrations is plotted according to salinity, a bell-shaped curve is obtained [9–17]. Most field and laboratory studies [8, 18] agree this is due to the desorption of particle-associated Cd triggered by the formation of chlorocomplexes.

The dissolved Cd peak is even more marked in macrotidal estuaries, where particle residence time is long and SM concentrations are very high.

Conversely, excess dissolved Cd (versus simple dilution) is minor or non-existent in microtidal estuaries such as the Rhone, Danube, or Lena rivers [19–22]. Similar situations can also be encountered in macrotidal estuaries during periods of low turbidity. Chiffoleau et al. [16] demonstrated that in the Seine estuary, virtually no dissolved Cd maximum exists when SM concentrations are low.

The solubilization of Cd in the estuarine environment is also governed by other more-or-less influential processes, i.e., early diagenesis in sediments, in particular in fine-matter deposit zones, and the dissolution of Cd associated with oxides (Fe, Mn) and/or organic matter in the turbidity maximum.

Due to its particular characteristics, Cd was chosen to “explore” the role of particle properties in the macrotidal estuary contaminant cycle.

This paper aims to explore the impact of particle surface properties (specific surface area, density of surface sites, acido-basic properties and complexation constant) – which we determined for three macrotidal estuaries (Seine, Loire, and Gironde) – on the behavior and speciation of “reactive” trace metals during estuarine transit.

We will be assessing this impact using a surface complexation model (MOCO) to reproduce Cd speciation during estuarine transit, taking into ac-

count the surface properties of particle samples taken from our three study estuaries in various scenarios.

2 Seine, Loire, and Gironde Estuaries: Main Characteristics

The functioning, morphology, and dynamics of our three study estuaries have already been extensively described in various works [4, 23–30]. Their main characteristics are recapped in Table 1.

The Seine catchment area alone represents approximately 40% of French economic activity and 30% of the French population. This estuary has undergone major successive engineering works and most of the downstream sections are dammed. The Seine estuary is the most highly anthropized of the three study estuaries, particularly compared with the Gironde estuary. The Gironde's catchment area features a very moderate population and degree of urbanization, meaning that it is close to a natural equilibrium.

The distribution of suspended matter measured during various cruises in the three estuaries [12, 13, 16, 31, 32] is shown on Fig. 2 as an example. This data highlights the space–time variability of SM distribution accord-

Table 1 Main morphologic and hydrodynamic characteristics [4, 23–30]

| | Seine | Loire | Gironde |
|--|--|--|---|
| Catchment surface area | $79 \times 10^3 \text{ km}^2$ | $115 \times 10^3 \text{ km}^2$ | $74 \times 10^3 \text{ km}^2$ |
| Tidal length | 160 km | 90 km | 170 km |
| River flow | $440 \text{ m}^3 \text{ s}^{-1}$ (average) $40 \text{ m}^3 \text{ s}^{-1}$ (min) $2500 \text{ m}^3 \text{ s}^{-1}$ (max) | $850 \text{ m}^3 \text{ s}^{-1}$ (average) $80 \text{ m}^3 \text{ s}^{-1}$ (min) $6000 \text{ m}^3 \text{ s}^{-1}$ (max) | $990 \text{ m}^3 \text{ s}^{-1}$ (average) $200 \text{ m}^3 \text{ s}^{-1}$ (min) $5000 \text{ m}^3 \text{ s}^{-1}$ (max) |
| Flushing time | 2–30 d | 1–20 d | Few days to several weeks |
| Particle residence time | Few days to several months | One week to several months | One to several months |
| Mean annual particulate discharge | $5 \times 10^5 \text{ t}$ | $1 \times 10^6 \text{ t}$ | $20 \times 10^6 \text{ t}$ |
| Average variation of SM concentrations | 1 mg L^{-1} – 2 g L^{-1} | 1 mg L^{-1} – 5 g L^{-1} | 1 mg L^{-1} – 10 g L^{-1} |

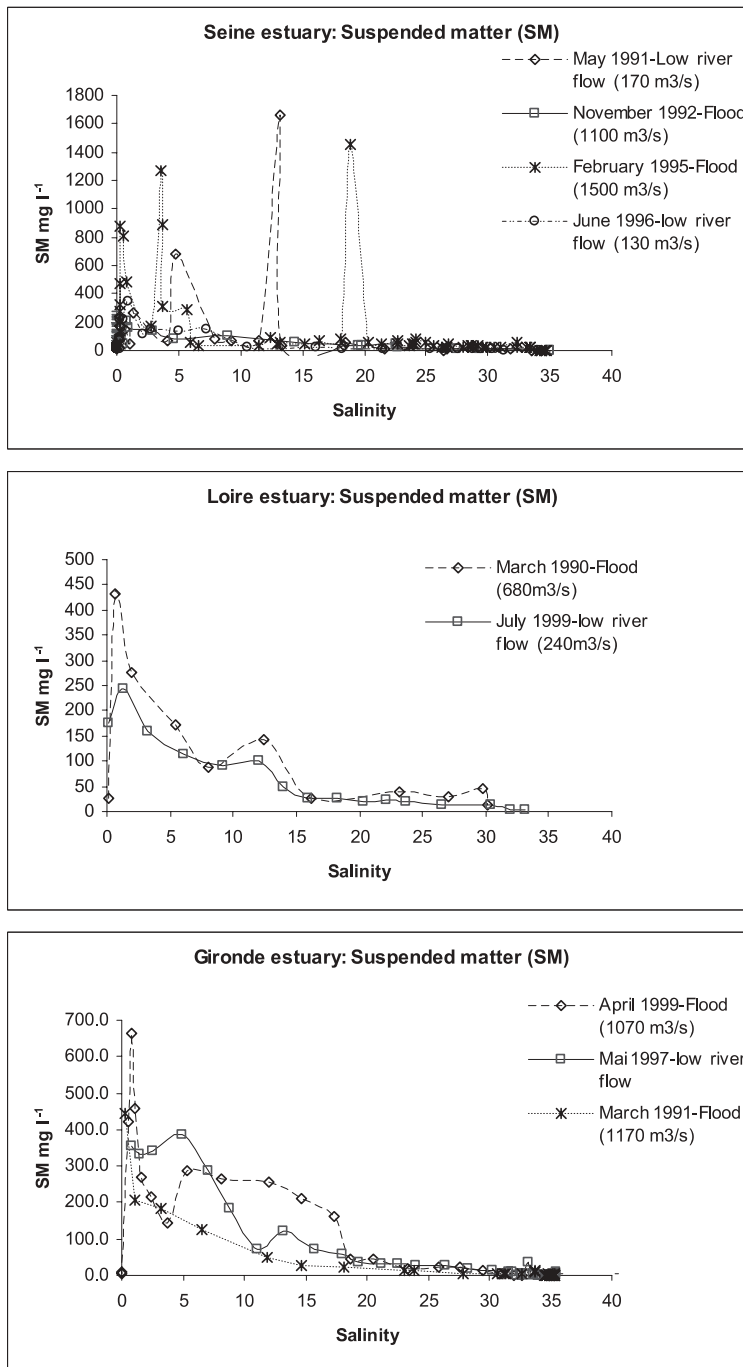


Fig.2 Distribution of suspended matter along the salinity gradient [12, 13, 16, 31, 32]

ing to salinity. Although these variations are due to multiple factors, the most influential are estuary shape, river flow, particulate input, and tidal conditions [6].

SM concentrations in the turbidity maximum may be as high as a few tens of milligrams per liter in surface waters and several grams per liter in bottom waters. According to the tidal coefficient, fluid mud lenses containing up to several hundred grams of SM per liter may be formed close to the bottom. This fluid mud layer, which can grow to a thickness of several meters, is subsequently subjected to accumulation and erosion cycles: it accumulates when the tidal coefficient drops and during neap tide, fractions into several lenses when the tidal coefficient rises, and erodes completely during spring tides [33].

3

Particle Geochemical Characteristics and Surface Properties

The geochemical and mineralogical characteristics of particles taken from the three study estuaries were determined in conjunction with an evaluation of parameters representing their surface properties. Most of this data, published by Boutier et al. [11, 12], Chiffoleau et al. [13, 16, 17], and Dange [30], is presented in Table 2.

Certain surface properties of natural particles – strongly related to their mineralogic characteristics – allow us to assess their reactivity in the aquatic environment. As most of these properties cannot be measured directly, they must be evaluated using various experimental approaches. The relevant parameters (Table 2), some of which will be used for simulations, are as follows: specific particle surface area (SA in $\text{m}^2 \text{g}^{-1}$); cation exchange capacity (CEC in mol g^{-1} of SM); total density of active surface sites ($[-\text{SOH}_{\text{tot}}]$ in mol g^{-1} of SM); mean intrinsic surface acid-base constants of these sites (K_{a1} and K_{a2}); and global intrinsic complexation constant (K_{m}) of these sites with regards to Cd.

The techniques implemented to evaluate these parameters and their limits are described in Gonzalez et al. [34] and Dange [30].

Briefly, the specific surface area of the particles is measured via nitrogen sorption using the BET method (Coulter SA 3100). Cation exchange capacity is estimated using ammonium as an exchangeable cation [35, 36].

The density of active surface sites and intrinsic surface acid-base constants of these sites (K_{a1} and K_{a2}) are evaluated using potentiometric acid-base titration (ABT). Surface acid-base constants are determined by adjusting the experimental data obtained by ABT using FITEQL 3.2 [30, 37–39].

The global intrinsic complexation constant of these sites with regards to Cd is obtained by experiments based on ^{109}Cd (particle samples taken throughout the estuary).

Table 2 Particle geochemical characteristics and surface properties: mean values and relative standard deviation (RSD)

| | Seine | | | Loire | | | Gironde | | |
|--|-------------------------|---------|----------|-------------------------|---------|----------|-------------------------|---------|----------|
| | Mean | RSD (%) | <i>n</i> | Mean | RSD (%) | <i>n</i> | Mean | RSD (%) | <i>n</i> |
| CaCO ₃ (%) | 26.8 | 13 | 24 | 7.9 | 11 | 5 | 8 | 3 | 11 |
| Al (%) | 3.4 | 32 | 45 | 7.7 | 28 | 25 | 8.9 | 20 | 30 |
| Fe (%) | 2.1 | 26 | 45 | 4.0 | 23 | 25 | 4.4 | 12 | 30 |
| Mn (μg g ⁻¹) | 479 | 27 | 45 | 1056 | 29 | 25 | 865 | 19 | 30 |
| COP (%) | 5.1 | 70 | 45 | 4.3 | 44 | 25 | 1.6 | 49 | 30 |
| SA (m ² g ⁻¹) | 6.0 | 32 | 21 | 22.8 | 20 | 6 | 37.2 | 17 | 11 |
| CEC (mol g ⁻¹) | 1.69 × 10 ⁻⁴ | 30 | 24 | 2.37 × 10 ⁻⁴ | 39 | 6 | 3.47 × 10 ⁻⁴ | 26 | 11 |
| [-SOH _{tot}] (mol m ⁻²) | 2.98 × 10 ⁻⁵ | 70 | 9 | 7.94 × 10 ⁻⁶ | 13 | 6 | 3.47 × 10 ⁻⁶ | 26 | 8 |
| <i>K</i> _{a1} | | | | 3.16 × 10 ⁻⁶ | 10 | 6 | 1.10 × 10 ⁻⁵ | 9 | 8 |
| <i>K</i> _{a2} | 2.57 × 10 ⁻⁵ | 13 | 10 | 1.91 × 10 ⁻⁷ | 8 | 6 | 3.80 × 10 ⁻⁷ | 7 | 8 |
| Log <i>K</i> _m | 0.48 | 52 | 7 | -1.51 | 45 | 4 | -1.21 | 22 | 5 |

Data from Boutier et al. [11, 12], Chiffolleau et al. [13, 16, 17] and Dange [3]

n number of measurements, *K*_{a1} and *K*_{a2} acidity intrinsic constants of surface sites, *K*_m “global” intrinsic stability constant of surface sites. These parameters are associated with equilibrium.

Gironde and Loire estuaries (single “average” type of amphoteric surface site):



Seine estuary (single “average” type of non-amphoteric surface site):



Surface complexation reaction in “average” sites:



The associated methodology is described in Dange [30].

Particles from the Seine estuary are characterized by their high carbonate and particulate organic carbon (POC) content. Loire and Gironde particles showed fairly similar characteristics, except for POC.

Relative standard deviation showed POC to be the most variable particle fraction in all three estuaries. Particles from the Gironde were the most homogeneous; this may be due to the fact that samples were taken exclusively from fluid mud, where the finest estuary particles homogenize.

Using this dataset, we then evaluated average particle mineralogic composition (calcite, quartz, organic matter, clays) [30]. Loire and Gironde particles were shown to have a similar composition, but Seine particles had a very high

carbonated fraction versus quartzose and argillaceous components due to the estuary's calcareous-type catchment area.

Seine particles were shown to have the lowest average specific surface area of the three particle types, due mainly to their large size [30]; they also had the lowest Al, Fe, and Mn concentrations, and a high carbonate content.

Cation exchange capacity is a function of the geochemical composition of particles, and in particular the characteristics of the clay minerals they contain. Gironde samples showed the highest values (Table 2), due to their high argillaceous content.

The density of active surface sites, and the proton exchange capacity (acidity constants) of these sites, can be evaluated using data from particle acido-basic titration. Seine particles had the highest density of surface sites, while Loire particles had approximately twice as many surface sites per square meter as Gironde particles. Despite the similar character of particles from the latter two estuaries, this could reflect the higher Mn and POC concentrations.

Experimental results have demonstrated that virtually no protons bind to Seine particles. Their global acido-basic properties are mainly controlled by the organic fraction of the particles and the carboxylic and phenolic functions (i.e., characteristic of the humic substances). Conversely, a significant quantity of protons bind to suspended matter in the Loire and Gironde estuaries.

The acido-basic properties of the particles can be modeled for two types of sites (Table 2): (i) amphoteric surface sites (hydroxyls), typical of sites associated with Fe and Mn oxy-hydroxides and with the argillaceous phase (fractions representing a significant proportion of Loire and Gironde particles), or (ii) non-amphoteric sites associated with the organic fraction, which largely control the acido-basic behavior of Seine particles.

Seine particle POC content is fairly similar to that of the Loire particles; the considerable differences observed in acido-basic behavior are actually due to the high argillaceous fraction of Loire particles.

These assumptions were tested by modeling experimental data (acido-basic titrations) using the FITEQL model [37] which enabled us to evaluate the acidity constants of the reactions studied (Table 2).

The data obtained showed Loire and Gironde particles to have very similar acido-basic properties, as suggested by their acidity constants (Table 2).

The K_{a2} value estimated for Seine samples is representative of carboxylic and/or phenolic sites, and confirms the predominant role of organic matter in the reactivity of these particles [30].

Depending on pH and total surface site density ($-\text{SOH}_{\text{tot}}$), the acidity constants of surface sites largely determine $-\text{SOH}$ site density (Eqs. 1, 2, 3 in Table 2), responsible for Cd surface complexation (Eq. 4 in Table 2). We obtain:

$$[-\text{SOH}] = [-\text{SO}^-][\text{H}^+]/K_{a2} \quad (5)$$

and

$$[-\text{SOH}] = [-\text{SOH}_2^+]K_{a1}/[\text{H}^+] \quad (6)$$

By calculating $-\text{SOH}_{\text{tot}} = [-\text{SOH}] + [-\text{SO}^-] + [-\text{SOH}_2^+]$, according to Eq. 5 and Eq. 6 we obtain:

$$-\text{SOH}_{\text{tot}} = [-\text{SOH}](1 + (K_{a2}/[\text{H}^+]) + ([\text{H}^+]/K_{a1})) \quad (7)$$

therefore:

$$[-\text{SOH}] = -\text{SOH}_{\text{tot}}/(1 + (K_{a2}/[\text{H}^+]) + ([\text{H}^+]/K_{a1})), \quad (8)$$

for amphoteric surface sites (i.e., Loire and Gironde particles).

For non-amphoteric sites (i.e. Seine particles), we obtain:

$$[-\text{SOH}] = -\text{SOH}_{\text{tot}}/(1 + (K_{a2}/[\text{H}^+])) \quad (9)$$

Adjustment of ^{109}Cd sorption data [30], whereby Cd sorption is considered as a formation of inner-sphere complexes (Table 2), enabled us to estimate the intrinsic complexation constant of surface sites in terms of Cd (K_m). Like most of the properties mentioned above, these constants were similar for Loire and Gironde particles. Seine particles showed the highest mean values.

In terms of sorption parameters, comparison with data collected in other works was problematic, as parameter values vary widely according to chosen experimental techniques and models (this is particularly true for acidity intrinsic constants and surface complexation constants). The comparison of values obtained in all three estuaries versus values estimated on particles from different environments gave comparable results [30]; any differences observed are largely due to particle mineralogic composition. In terms of Cd, the complexation constants of particles of various origins obtained using a similar modeling technique were compiled by Muller and Duffek [40]. In our study, Loire and Gironde complexation constants were comparable to compiled data.

4

Behavior of Cd in Macrotidal Estuaries

Contamination by trace metals, and their behavior in the three estuaries, has been widely studied [10–17, 32, 34, 41, 42].

The high physicochemical gradients encountered in the estuarine environment (suspended matter, salinity, pH, and major elements) are responsible for the phase changes undergone by Cd during its oceanward transit.

The majority of macrotidal estuaries experience a rise in dissolved Cd concentrations as soon as salinity rises, followed by a drop in highly saline waters [9–17].

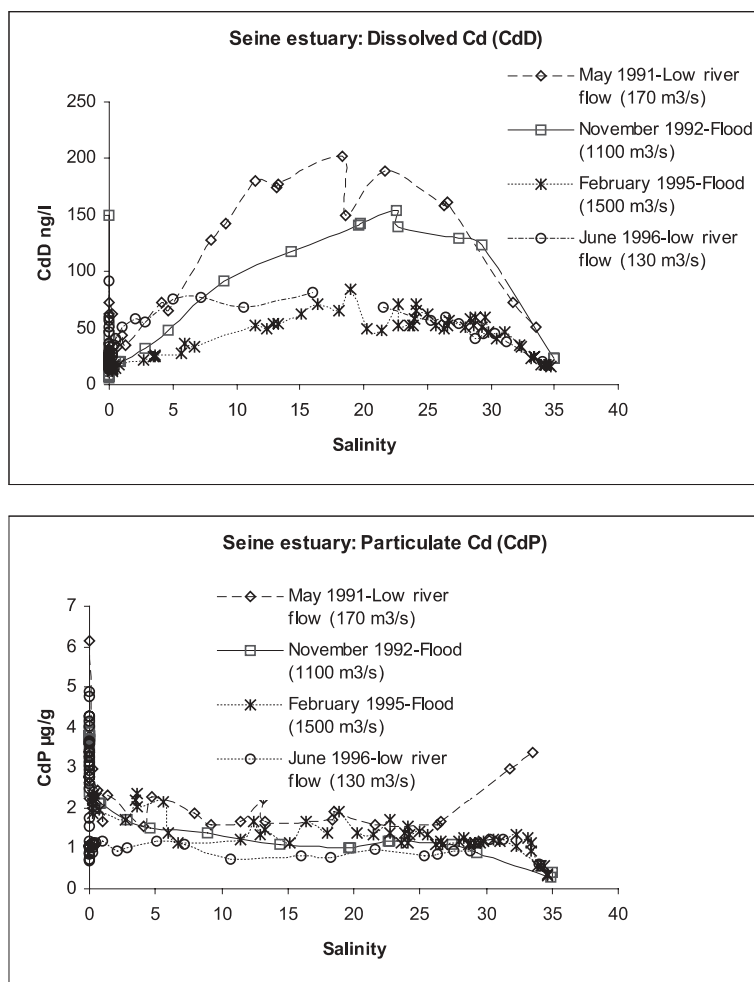


Fig. 3 Dissolved and particulate Cd in the Seine estuary [13, 16]

Maximum dissolved Cd can be studied with various flow regimes and in different seasons within the same estuary. To illustrate this point, the distribution of dissolved and particulate Cd corresponding to the previously illustrated SM profiles is presented in Figs. 3, 4, and 5.

We observed this typical behavior in our study estuaries, crystallized by a more-or-less visible “dissolved Cd bump”. Variations in the scope of this phenomenon within one or several estuaries may be conditioned by several factors: flow rates, Cd concentrations at the upstream and downstream limits, contamination levels, the size of the turbidity maximum and its position versus the salinity gradient, or particle sorption properties. This paper aims to examine the impact of the latter two factors.

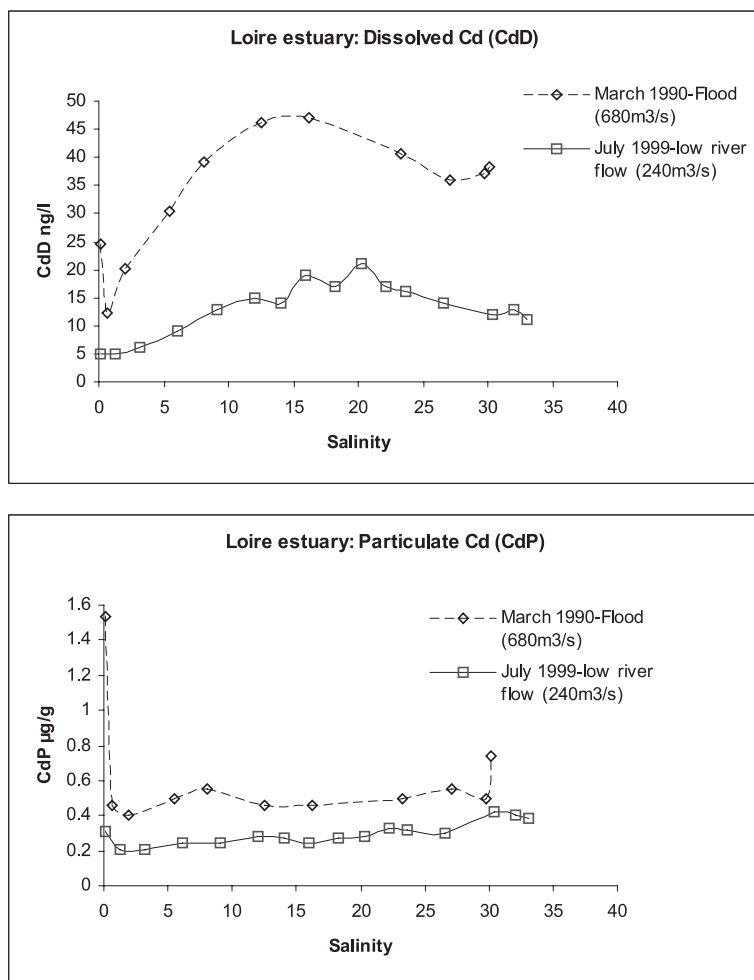


Fig. 4 Dissolved and particulate Cd in the Loire estuary [12]

Temporal variations in Cd fluxes entering the estuary, or the presence of a sporadic Cd source, could explain the dissolved Cd bump. But the majority of studies assign this characteristic evolution (bell-shaped curve) to Cd desorption from particles entering the estuary, caused by the formation of highly stable dissolved chlorocomplexes when chlorinity (salinity) rises. This hypothesis was confirmed by laboratory experiments in which ^{109}Cd was added to samples of raw river water (dissolved phase + particles) mixed with raw water taken from the open sea [8, 18]. Turner [8] demonstrated that the Cd partition coefficient (K_d) in various estuaries evolves as a function of salinity. K_d differs widely with low salinity in the three study estuaries due to variations in the characteristics of particles enter-

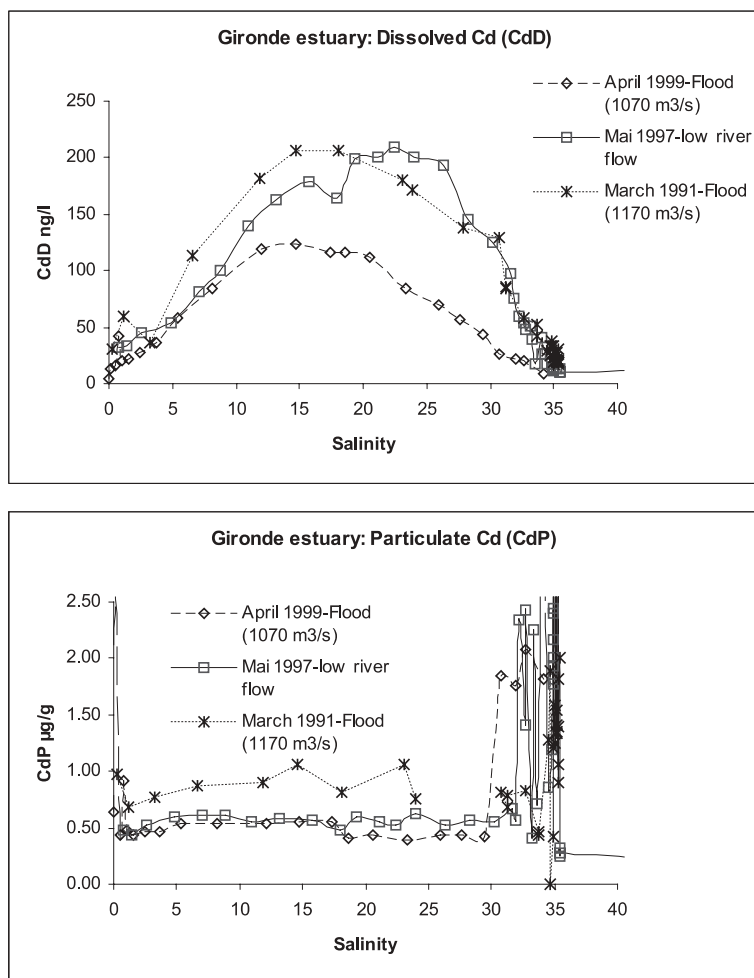


Fig. 5 Dissolved and particulate Cd in the Gironde estuary [31, 32]

ing the estuary and river water composition. But K_d evolution as a function of salinity remains similar, and merges to comparable values when salinity is high.

Interestingly, some campaigns (Figs. 3, 4, and 5) have observed high particulate Cd concentrations associated with high salinity (up to $3 \mu\text{g g}^{-1}$ in the Seine estuary). This seemingly contradictory behavior is generally thought to be associated with high chlorophyll *a* concentrations [12, 16, 32], and may suggest that particles of phytoplanktonic origin could have powerful Cd sorption properties.

The global behavior of Cd at the fresh/salt water interface means that macrotidal estuaries can flush significant amounts of dissolved Cd into adja-

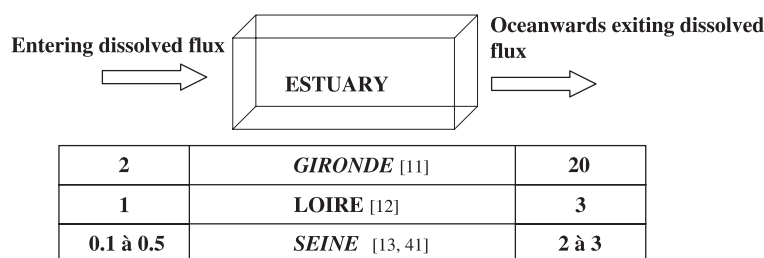


Fig. 6 Impact of estuarine processes on oceanwards Cd fluxes (in t year^{-1}) [11–13, 41]

cent coastal waters. Figure 6 illustrates the extent of this phenomenon, which actually reflects the differences in quantities of dissolved Cd entering and exiting the estuary.

In Table 3, ^{CE}_b mean dissolved Cd concentrations in estuarine waters are compared with likely concentrations in various other aquatic environments.

On the whole, concentrations near the coast are higher than those in the ocean; this underlines the fact that Cd inputs are primarily of continental origin. The differences in surface water and bottom water concentrations pinpointed in the Atlantic and Pacific Oceans illustrate the “nutrient-like” be-

Table 3 Dissolved Cd concentrations (ng L^{-1}) in various aquatic environments

| | | | |
|------------------------------|-----------------------------|--------------|----------|
| Oceanic waters | Atlantic | 10–45 | [43] |
| | Pacific | 80–110 | [43] |
| Surface waters | Arctic | 7–33 | [44] |
| | Atlantic | 0.2–16 | [44] |
| | Pacific | 3–67 | [44] |
| Coastal and estuarine waters | Marennes-Oléron Bay | 13–23 | [44] |
| | Gironde estuary | 10–393 | [45] |
| | Loire estuary | 11–61 | [10, 11] |
| | Rhône (microtidal) estuary | 48 (average) | [12] |
| | Seine estuary | | [10] |
| | Upstream limit (Poses weir) | 5–73 | [41] |
| | Estuary | 5–202 | [16, 17] |
| | Scheldt estuary | 450 (max) | [46] |
| Porewaters | Hudson estuary | 618 (max) | [47] |
| | St-Laurent estuary | 6–582 | [48] |
| | Fjord | < 10 | [49] |
| | Equatorial Pacific | 112–267 | [50] |
| | Californian Shelf | 12–280 | [51] |
| | Marennes-Oléron Bay | 4–170 | [52] |
| | West-Gironde mud patch | 60–400 | [52] |
| Seine (intertidal mud patch) | 19–1328 | [53] | |

^{CE}_b Author: Is there a figure missing for the Seine estuary?
Please check that refs are correct

havior of Cd. Differences in average concentrations in Atlantic and Pacific waters are owed to the fact that Pacific waters are older.

Concentrations within each estuary are extremely variable and characterized by wide space–time variations related mainly to hydrodynamics. Catchment area characteristics and variations in inputs of anthropic origin can lead to widely differing mean concentrations between estuaries.

In porewaters, the concentrations are very variable, even within the same environment. These concentrations are controlled by the speciation of the particulate Cd which integrates the sedimentary column and of the diagenetic conditions which in the sediments vary temporally and according to the depth.

With the aim of correlating the degree of contamination of various estuaries, Table 4 offers a comparison of unindustrialized estuaries (Amazon, Lena), featuring minimal observable concentrations, versus a selection of European and American estuaries of various sizes, with differing degrees of contamination.

These comparisons are questionable, however, as the various cruises took place at different and sometimes far-distant periods. In addition, the majority of cruises were one-offs (one cruise lasting a few days), whereas others involved pluriannual monitoring. Finally, even if identical techniques and strategies are used, it is still difficult to draw firm conclusions by comparing concentrations in various sites. For example, comparing maximum dissolved Cd in the Gironde and Seine estuaries could lead us to conclude that the Gironde is far more contaminated by Cd than the Seine, whereas measurements of particulate Cd in the turbidity maximum suggest the contrary. The explanation for this lies in the different characters of estuary particles, e.g., Seine particles are much richer in carbonates and organic matter than the highly argillaceous Gironde particles, and hence have different sorption capacities. This hypothesis is corroborated by the particle characteristics presented above.

The data presented in Table 4 with the aim of characterizing estuary contamination shows that:

- Dissolved and particulate Seine concentrations at Poses weir (upstream limit) are actually higher than the minimum levels previously described in the literature. They largely exceed levels in the Loire estuary, which can be considered as an example of a little-contaminated European estuary.
- Measurements at Poses weir are in the same range as those observed in the Gironde or Scheldt estuaries, known to be contaminated by Cd.
- The particulate Cd content of the Seine mixing zone is very high versus other estuaries. Only the Scheldt has higher levels.
- Maximum dissolved Cd measured in the Seine fresh–salt water mixing zone is very high versus the Lena, Amazon, or Loire. For the past 5 years, it has been similar to Gironde levels.

Table 4 Cd concentrations in various estuaries

| | Upstream zone | | Downstream zone (mixing zone) | | Refs. |
|-------------|-------------------------------|--------------------------------|-----------------------------------|--------------------------------|--------------|
| | Cd D (ng L ⁻¹) | Cd P (mg kg ⁻¹) | Max Cd D (ng L ⁻¹) | Cd P (mg kg ⁻¹) | |
| Amazon | 50 | | | | [9] |
| Lena | 3–12 | | 34 | | [20] |
| Mississippi | 18–20 | | 33 | | [54] |
| St Laurent | 11–16 | 0.3–5 | 25 | 0.2–0.5 | [55] |
| Scheldt | 20 | 8.8 | 90 | 3.7 | [56] |
| Ebre | 40 | 5.8 | | | [57] |
| Rhône | | | | | |
| 1995 | 5–38 | 0.2–1.5 | | | [58] |
| 1996 | | 55 | 0.8 | | [19] |
| Loire | 24 | 1.5 | 60 | 0.47 | [12] |
| Gironde | | | | | |
| 1984–1985 | 20–100 | 6–14 | 400 | 1 | [11] |
| 1994 | 40–70 | 1.8–7 | 130 | 0.53 | [14] |
| Seine | | | | | |
| 1990–1992 | 5–73 | 2.8–7.2 | 202 | 1.7 | [41] |
| 1994–1998 | 5–87 | 1.3–12 | 82–127 | 0.8–1.5 | [16, 17, 42] |

(Cd D dissolved Cd, Cd P particulate Cd)

The Seine estuary can hence be classified as one of the most highly Cd-polluted estuaries.

In our comparison (Table 4), average Cd concentrations in suspended matter in both the upstream and mixing zones are significantly higher in the Seine estuary than in the other study estuaries. There may be several reasons for this: the fraction of Cd associated with the crystalline phase may be larger because of geological reasons, higher sorption capacity (as per estimated K_m values), or higher Seine contamination, contrary to the data shown in Table 4 (especially when compared with dissolved Cd concentrations measured in the Gironde estuary).

These various “possibilities” must, in some way, be responsible for measured particulate Cd concentrations. The purpose of this paper is to assess the impact of particle characteristics and behavior, through the study of sorption properties.

5

Presentation of the Model and Simulation Conditions

We used a surface complexation model (MOCO) to highlight the role of particle surface properties (specific surface area, density of surface sites, acido-

basic properties, complexation constant) in Cd speciation in the macrotidal estuarine environment. This model had already been used to simulate Cd behavior in the three study estuaries. In our previous studies [34, 59], model results were compared with the numerous dissolved and particulate Cd measurements performed in situ. The model has also previously been applied to other metal cations such as Co, Cs, and Hg [30, 60].

This type of model considers Cd sorption to particles as a formation of complexes with functional surface groups [34, 61–64]. Dissolved and particulate Cd species are computed by solving equilibrium equations incorporating various dissolved ligands and particles simultaneously. Included dissolved ligands are chlorides, hydroxides, and sulfates. Complexation constants are derived from Comans and Van Dijk [18].

Table 5 shows the reactions processed by the model.

For the purposes of this study, particles were considered “globally” (use of mean sorption properties evaluated from particles from the various estuaries shown in Table 2). This type of approach assumes that the various

Table 5 Reactions processed by the MOCO model to simulate Cd speciation

| | Log K | |
|--|----------------------|---|
| $\text{Cd}^{2+} + \text{Cl}^- = \text{CdCl}^+$ | 2.0 | $[\text{Cl}^-]$ calculated from salinity |
| $\text{Cd}^{2+} + 2\text{Cl}^- = \text{CdCl}_2$ | 2.6 | |
| $\text{Cd}^{2+} + 3\text{Cl}^- = \text{CdCl}_3^-$ | 2.4 | |
| $\text{Cd}^{2+} + 4\text{Cl}^- = \text{CdCl}_4^{2-}$ | 1.7 | |
| $\text{Cd}^{2+} + \text{OH}^- = \text{Cd}(\text{OH})^+$ | 3.9 | $[\text{OH}^-]$ calculated from pH |
| $\text{Cd}^{2+} + 2\text{OH}^- = \text{Cd}(\text{OH})_2$ | 7.6 | |
| $\text{Cd}^{2+} + 3\text{OH}^- = \text{Cd}(\text{OH})_3^-$ | 8.7 | |
| $\text{Cd}^{2+} + 4\text{OH}^- = \text{Cd}(\text{OH})_4^{2-}$ | 8.6 | |
| $\text{Cd}^{2+} + \text{SO}_4^{2-} = \text{CdSO}_4$ | 2.4 | $[\text{SO}_4^{2-}]$ calculated from salinity |
| $\text{Cd}^{2+} + 2\text{SO}_4^{2-} = \text{Cd}(\text{SO}_4)_2^{2-}$ | 3.4 | with presumed conservativity |
| $\text{Cd}^{2+} + 3\text{SO}_4^{2-} = \text{Cd}(\text{SO}_4)_3^{4-}$ | 3.1 | |
| $\text{Cd}^{2+} + 4\text{SO}_4^{2-} = \text{Cd}(\text{SO}_4)_4^{6-}$ | -0.7 | |
| Surface reactions: Cd sorption to the surface of a “global” particle. Apparent stability constants were calculated from intrinsic constants _(int) , taking into account the electrostatic effects of the surface charge as estimated by the Gouy-Chapman model. | | |
| $\text{S} - \text{OH}_2^+ = \text{S} - \text{OH} + \text{H}^+$ | $K_{a1(\text{int})}$ | $K_{a1(\text{int})}$ and $K_{a2(\text{int})}$ are the acidity constants determined experimentally |
| $\text{S} - \text{OH} = \text{S} - \text{O}^- + \text{H}^+$ | $K_{a2(\text{int})}$ | |
| “Global” particle | | |
| $\text{S} - \text{OH} + \text{Cd}^{2+} = \text{S} - \text{OCd}^+ + \text{H}^+$ | $K_{m(\text{int})}$ | $K_{m(\text{int})}$ is determined experimentally |

Complexation of cadmium with various dissolved ligands: Each equilibrium is defined by a complexation constant (stability constants) for each dissolved complex derived from Comans and Van Dijk [18]. Values at 25 °C are used (no temperature correction). The activity coefficients of the various species are calculated using the Davies equation

reactions reach equilibrium quasi-instantaneously, and that they are completely reversible.

The choice of modeled processes was based on studies on Cd biogeochemistry in the estuarine environment, which suggest that most Cd behavior can be explained by its stability in the form of chlorocomplexes and rapid desorption during estuarine transit [11, 14, 18, 65].

A fuller description of the model, including parameter selection methods and validation for the various study estuaries, was published previously [30, 34, 42, 59].

We simulated various particle distribution scenarios within a given estuary, using the surface properties of particles taken from the three study estuaries. These “classic” scenarios (Fig. 7) were defined on the basis of suspended matter distribution measurements according to salinity, presented in Fig. 2.

The distribution of SM concentrations in the three study estuaries (Fig. 2) can be roughly grouped into three scenarios: migration of the turbidity maximum towards the highest salinities, the presence of a second, smaller and more “thinly spread” turbidity maximum, and very high SM peaks within the estuary (Fig. 7). These scenarios were used as the basis for our simulations.

The required input data was as follows (Table 5):

- Concentrations of the various included dissolved ligands: chlorides (calculated on the basis of salinity), hydroxides (calculated on the basis of pH, which will be considered as equal to 7.8 throughout the estuary), sulfates (calculated on the basis of salinity, considered as conservative and based on concentrations of 3×10^{-4} M and 0.02 M at the river and ocean boundaries, respectively)
- SM concentrations in our classic situations (Fig. 7)
- Parameters representing the surface properties of natural particles (Table 2).

All simulations used mean sorption parameter values (SA , $[-SOH_{tot}]$, K_{a1} , K_{a2} and K_m), evaluated for particles from the three study estuaries. To test the natural variability of these parameters within the same estuary, we also did simulations taking into account standard deviation from mean values (Table 2).

The model computes concentrations of various species (dissolved and particulate) at equilibrium (Table 5) for a given total Cd concentration.

We chose a total Cd concentration of 10^{-9} M, which is representative of data collected in the three study estuaries.

For greater clarity, the various dissolved Cd species (free Cd and Cd complexed with chlorides, sulfates, or hydroxides) are not shown.

The results are expressed as a percentage of total dissolved Cd (sum of all dissolved species calculated by the model, see Table 5).

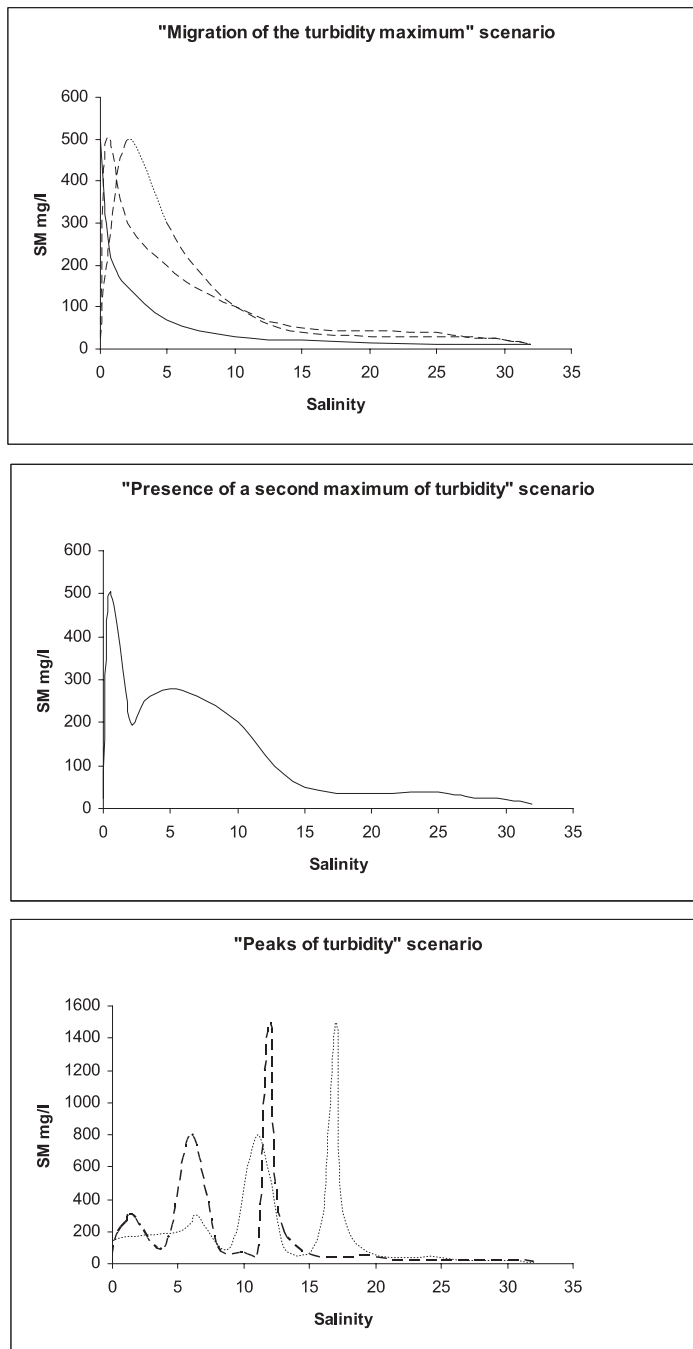


Fig. 7 Typical scenarios defined according to the distribution of suspended matter versus salinity (measurements presented in Fig. 2)

6 Results and Discussion

6.1 Global Sorption Capacity of Particles (GSC)

Particle sorption capacity depends on: the exchange capacity of protons in surface sites, ascertained using acidity constants K_{a1} and K_{a2} ; total surface site concentrations and specific particle surface areas; and the complexation constant of surface sites in terms of Cd.

In order to compare the sorption characteristics of particles from the three study estuaries, and interpret the results obtained, we evaluated their global sorption capacity (GSC). For this purpose, -SOH site concentration (in mol L^{-1}) was computed with various salinities, at constant pH of 7.8 (corresponding to the simulation pH) and a constant SM concentration (100 mg L^{-1}). We based our calculation on the sorption parameters (mean, minimum, and maximum) of each particle type (Table 2), i.e., specific surface area, density of surface sites, and acid-base constants of these sites (K_{a1} and K_{a2}).

The concentration of “complexating” surface sites (Eq. 4, Table 2) thus obtained was multiplied by the global intrinsic complexation constant of the study sites in terms of Cd.

This parameter is a good indicator of the importance of the particles sorption capacities and it makes it possible to compare particles of different nature.

According to our results (Fig. 8), Loire particles possess the highest concentrations of complexating surface sites due to their acidity intrinsic properties. Seine particles have the lowest concentrations, as their surface sites are non-amphoteric (Eq. 3, Table 2).

Computing GSC with respect to Cd underlined the impact of the surface site complexation constant. The high value of this constant in Seine particles means that despite a very weak concentration of complexating sites, computed GSC reactivity was similar to that obtained for the other two particle types (Fig. 8).

Differences exceeding one order of magnitude were observed in GSC computed on the basis of average, minimum, or maximum sorption parameters. Using average and maximum parameters, Loire particles were shown to have the highest GSC, whereas Gironde particles had the GSC highest global reactivity using minimum parameters. The reactivity of Seine particles was very similar to that of Gironde particles using average parameters, and similar to Loire particles using maximum parameters. Interestingly, using average and maximum parameters, Seine particles had the highest GSC with zero salinity; reactivity decreased very strongly when salinity increased, and was similar to that of the other particles at around salinity 1.

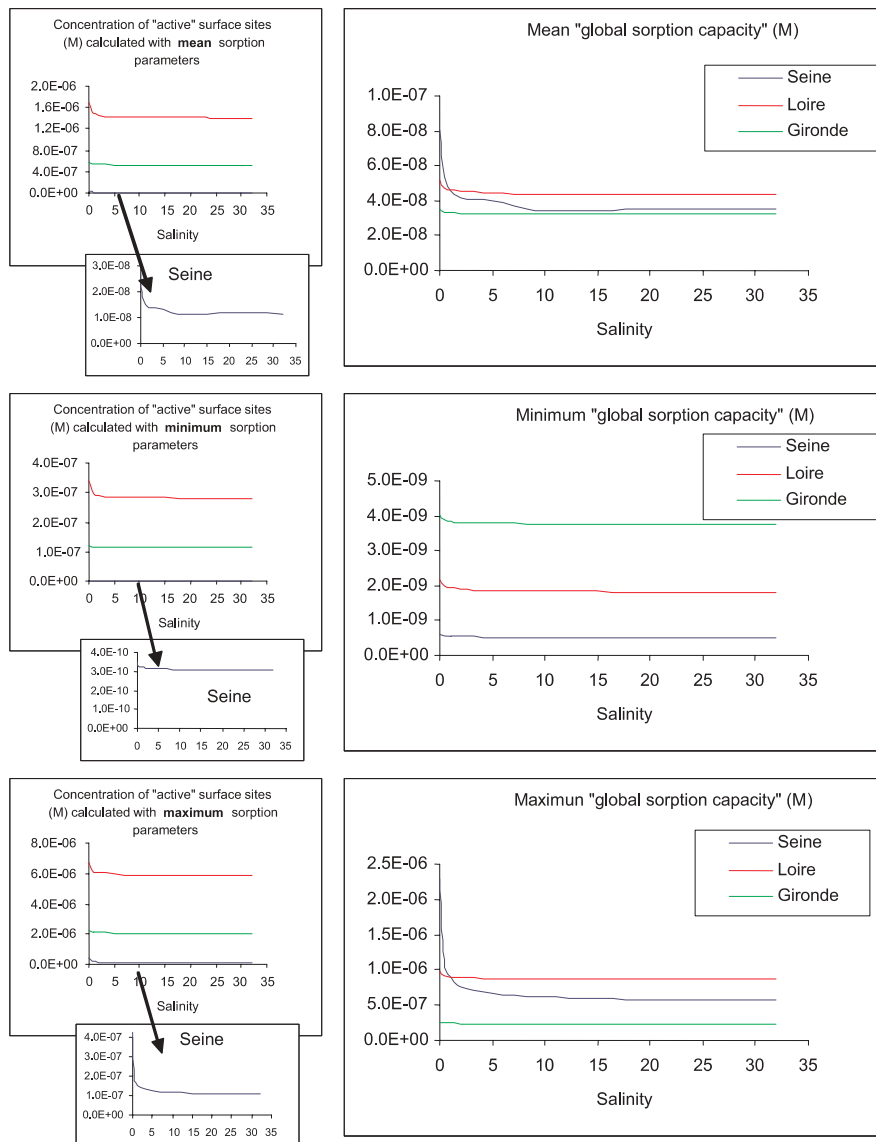


Fig. 8 Concentration of "reactive" surface sites and "global sorption capacity" of particles (see text)

This phenomenon stems from the fact that Seine particle surface sites are non-amphoteric (Eq. 3, Table 2). Salinity increases cause conditional equilibrium constants (K_{a1} , K_{a2}) to rise, due to a drop in activity coefficients (this drop is most significant at an ionic force of zero to a few hundredths). According to Eq. 9, when pH is constant, the increase in K_{a2} leads to a reduction

in sites capable of complexing Cd. This reduction increases as K_{a2} value is low. As a result, using average and maximum parameters, the GSC of Seine particles was far greater when salinity neared zero, whereas practically no difference was observed with other particle types. In the case of the Loire and the Gironde (amphoteric sites), the increase in K_{a2} when salinity rises is countered by that of K_{a1} (Eq. 8); the phenomenon is therefore virtually non-existent.

The comparison of GSC values shows that within the same estuary the differences (between the average, minimum, and maximum values) can be very significant. These differences are the result of the space and temporal variations of the nature of the particles.

6.2

Simulation of Migration of the Turbidity Maximum

Migration of the turbidity maximum, according to flow rates and tidal conditions, and within a relatively weak salinity range, is frequently encountered in macrotidal estuaries.

Using average properties, the results obtained were virtually identical notwithstanding particle type (Fig. 9), in particular for the Seine and Loire estuaries. Differences were significant with zero salinity and a low SM content (25 mg L^{-1}). As observed in the evaluation of GSC, Seine particles were shown to have far greater sorption properties with zero salinity.

With minimum parameters (Fig. 10), all Cd is considered to be in dissolved form, notwithstanding particle type, except in zones where SM concentrations are high (characterized by minimal %CdD values). Despite the major differences in GSC (Fig. 8) resulting from reduced sorption capacities, differences in Cd partition were negligible except in the turbidity maximum. Differences in particle origin were nil when salinity reached 5.

Using maximum sorption parameters (Fig. 11), the evolution of dissolved Cd percentages according to salinity was virtually the same for Seine and Loire particles, whose global reactivity is comparable. Dissolved Cd percentages were highest with Gironde particles, which are characterized by the lowest GSC. The turbidity maximum had a very marked impact in comparison to previous simulations, with extremely low dissolved Cd percentages at salinities of 0–5, in particular for Seine and Loire particles. Unlike in the simulations using average or minimum properties, we observed significant differences in dissolved Cd percentages even when salinity was high. This is due to the fact that chloride impact is weakened when particle sorption capacity rises. As for average properties, a shift in maximum dissolved Cd (around 80% for Gironde particles and 60% for Loire and the Seine particles) was observed with higher salinities and migration of the turbidity maximum.

To illustrate this scenario, our simulation results are also shown in terms of concentrations (Figs. 12–14).

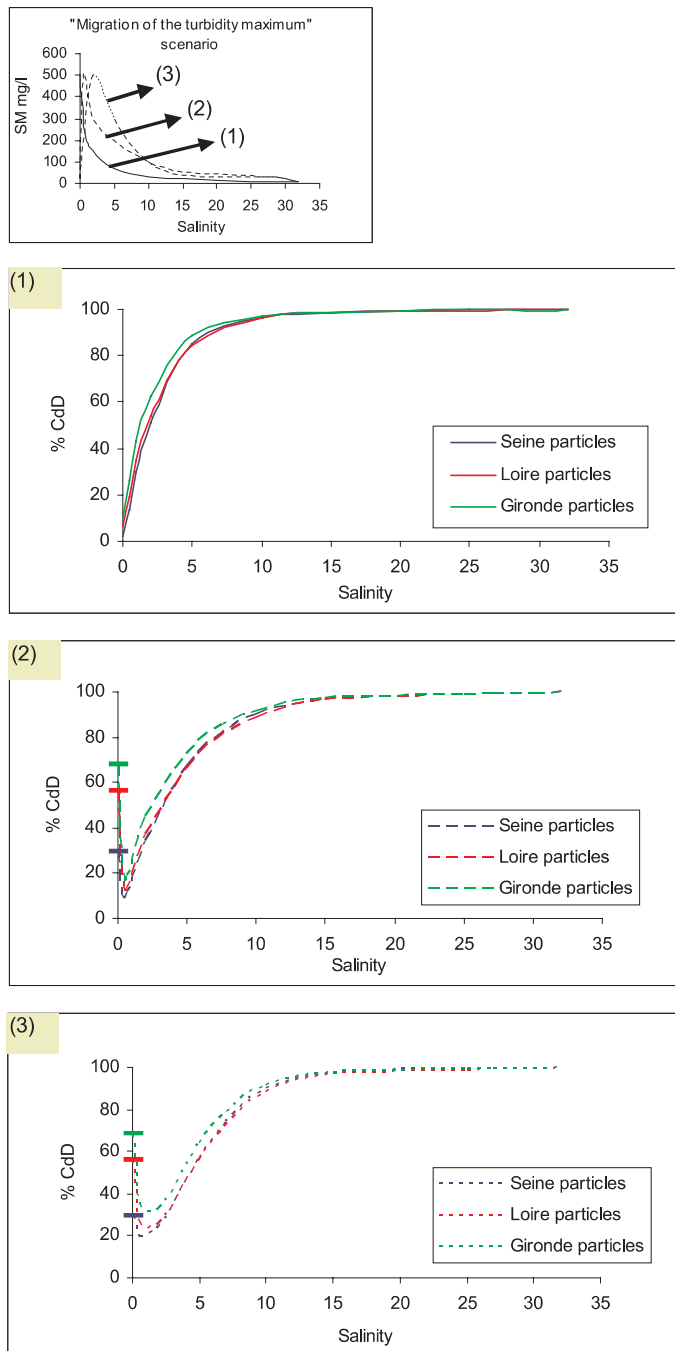


Fig.9 Percentage of dissolved Cd (%CdD): "Migration of the turbidity maximum" scenario. Mean sorption properties simulation

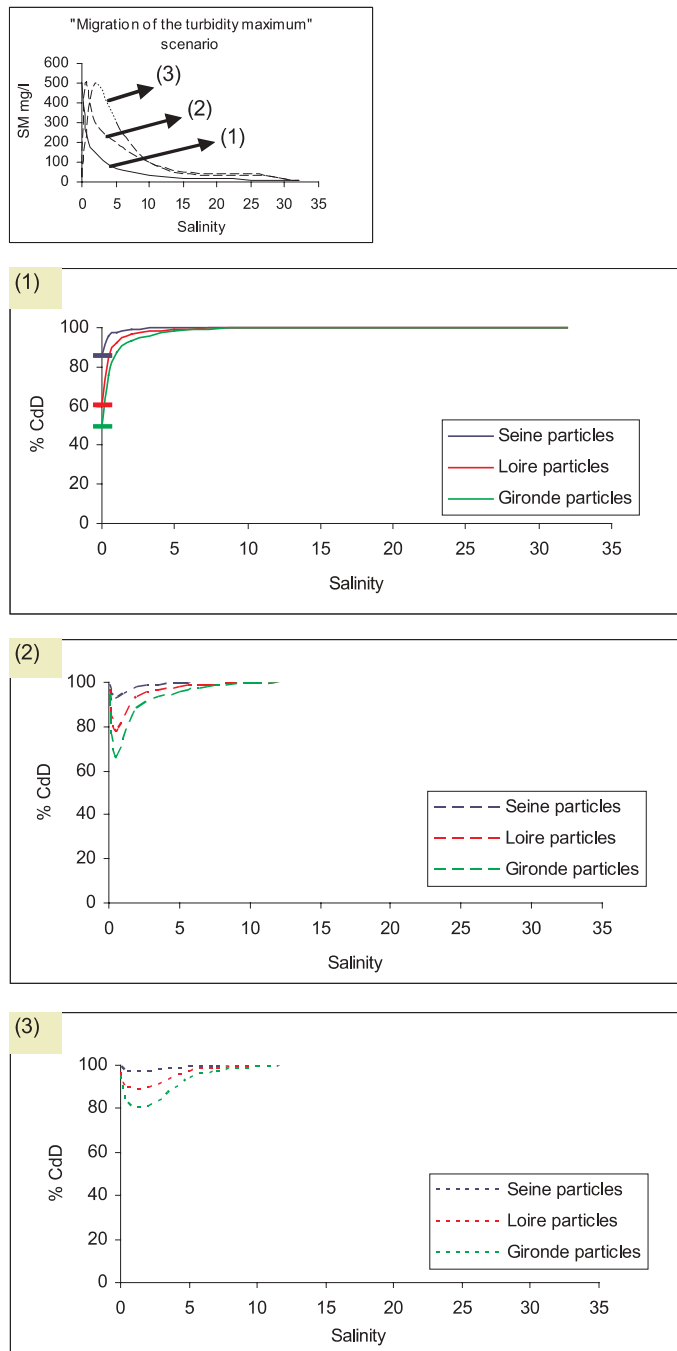


Fig. 10 Percentage of dissolved Cd (%CdD): "Migration of the turbidity maximum" scenario. Minimum sorption properties simulation

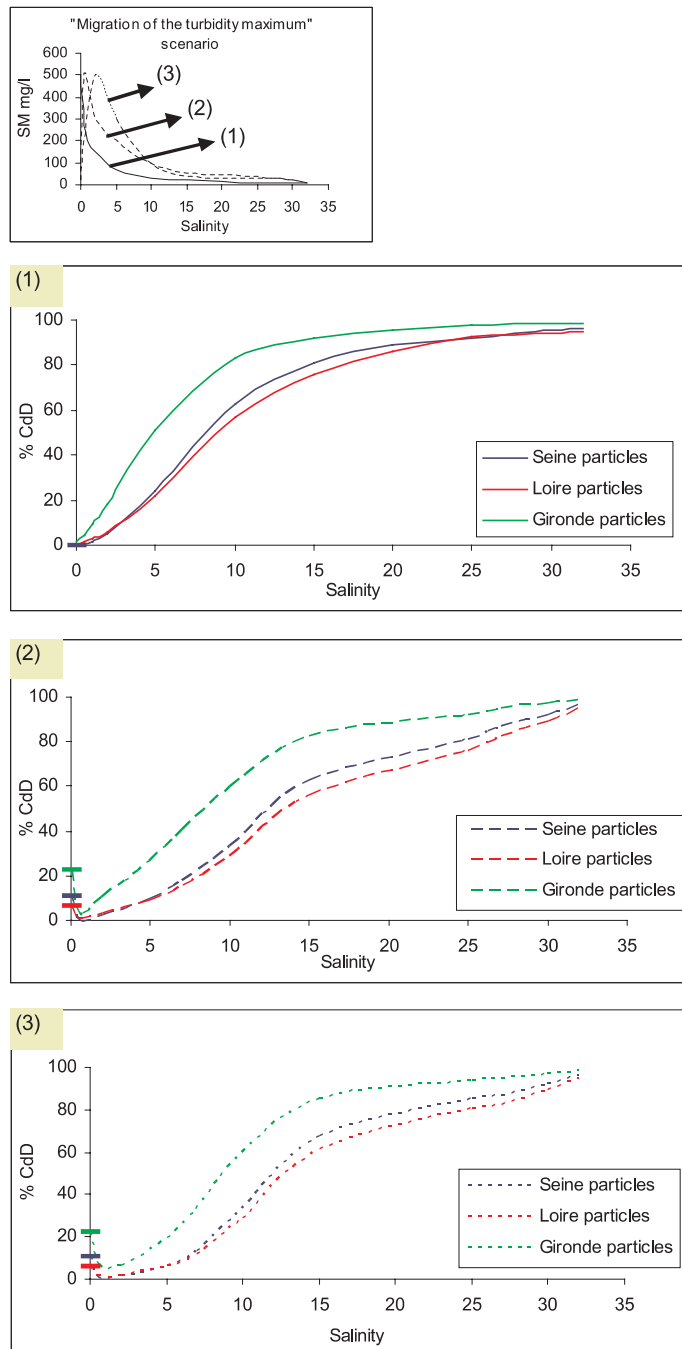


Fig. 11 Percentage of dissolved Cd (%CdD): "Migration of the turbidity maximum" scenario. Maximum sorption properties simulation

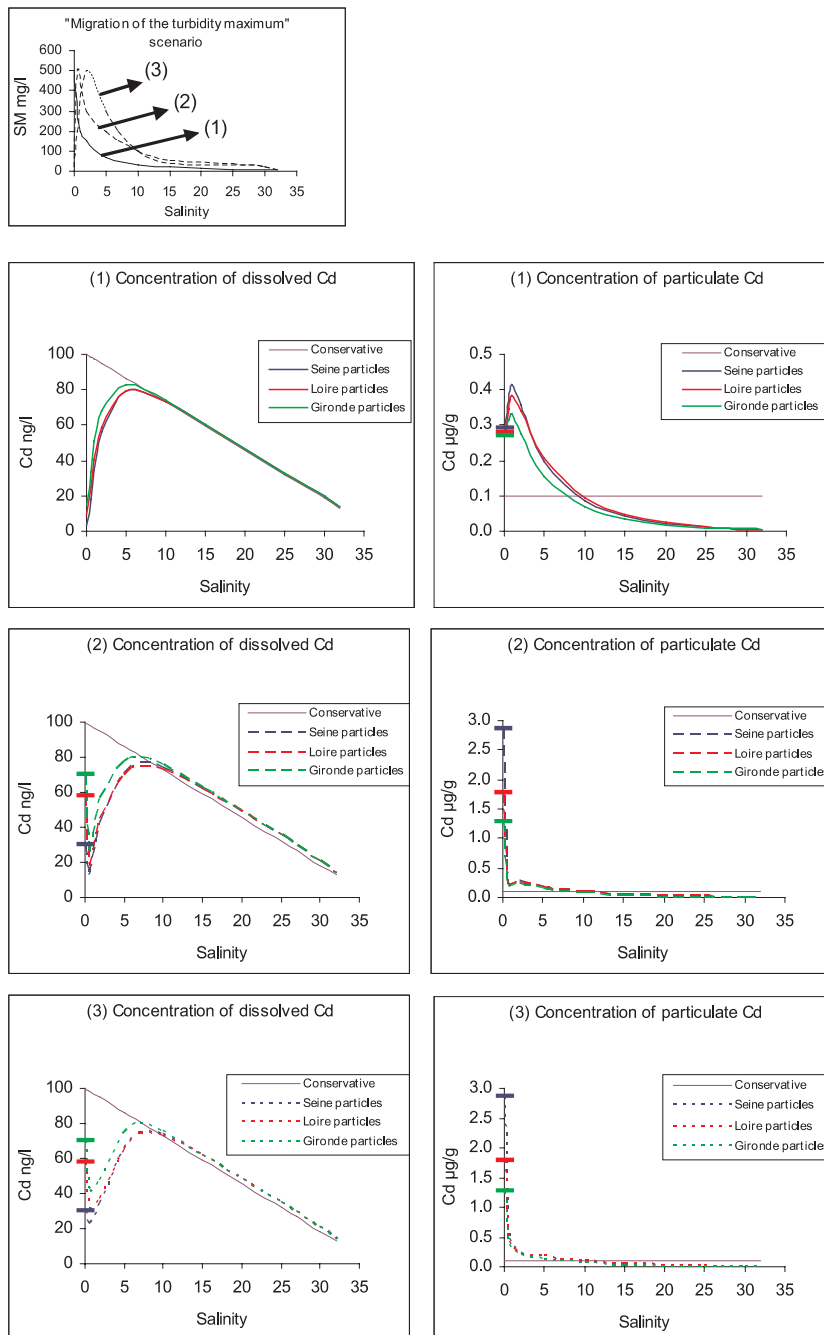


Fig. 12 Concentration of dissolved and particulate Cd: "Migration of the turbidity maximum" scenario. Mean sorption properties simulation

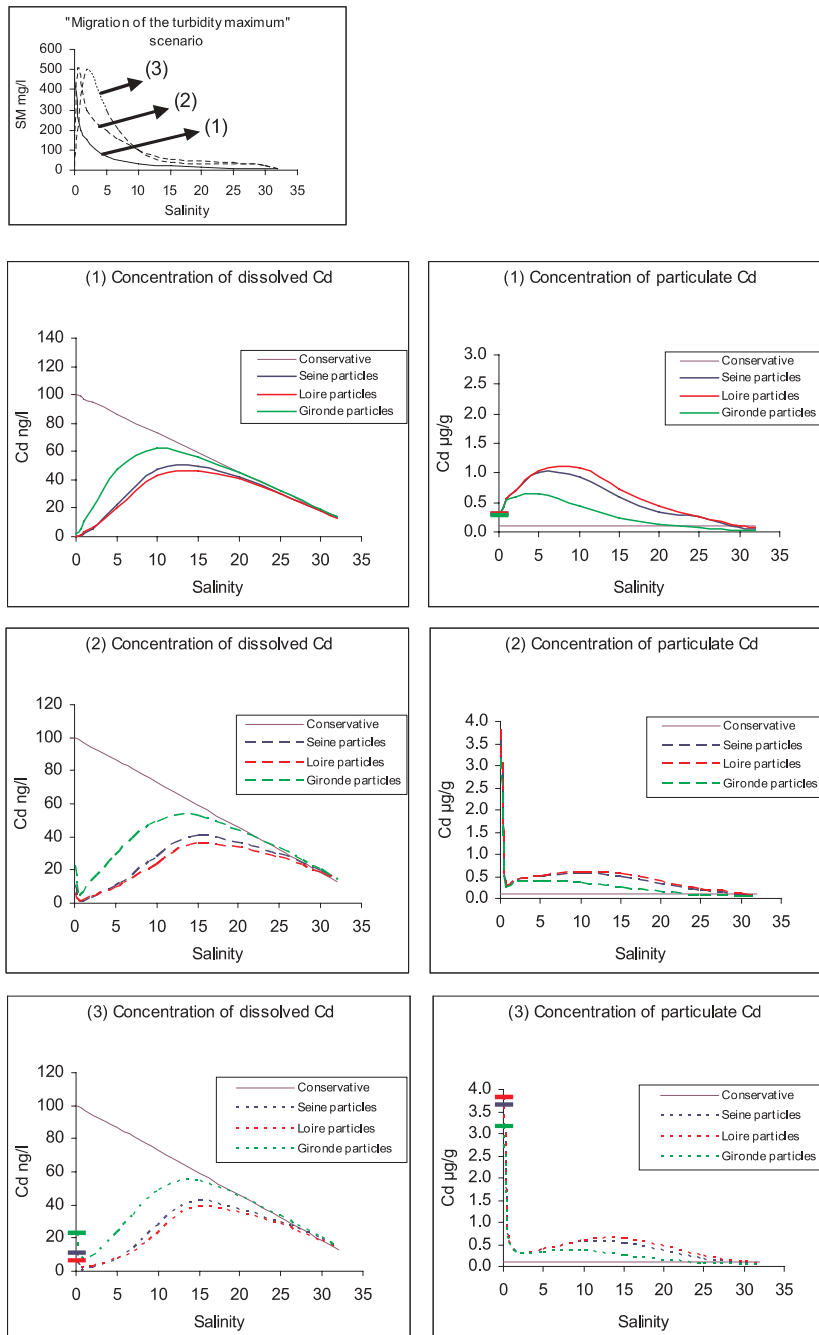


Fig. 13 Concentration of dissolved and particulate Cd: "Migration of the turbidity maximum" scenario. Maximum sorption properties simulation

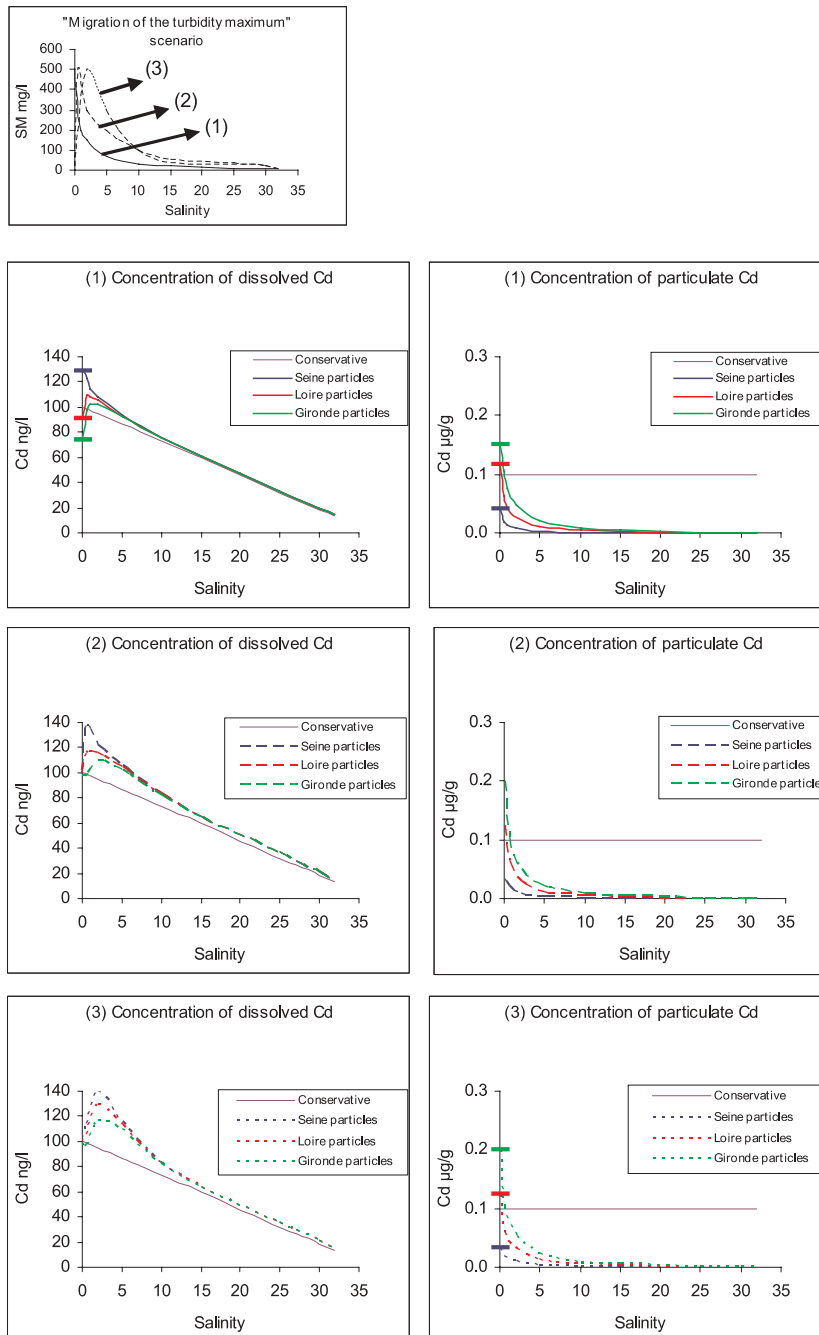


Fig. 14 Concentration of dissolved and particulate Cd: "Migration of the turbidity maximum" scenario. Minimum sorption properties simulation

For the purpose of these simulations, we used the following dissolved Cd concentrations: 100 ng L^{-1} at the upstream limit (0 salinity) and 5 ng L^{-1} at the marine boundary (salinity 35). In terms of particulate Cd, particles entering the estuary were considered as having an adsorbed Cd concentration of $0.1 \mu\text{g g}^{-1}$. The model divides “total” Cd into various species (Table 5) for a given salinity. Total Cd is calculated on the basis of SM, sorbed Cd, and dissolved Cd concentrations.

Particulate cadmium computed by the model only represents the fraction adsorbed to the surface of particles. This fraction cannot be compared directly with total particulate cadmium concentrations measured in the study estuaries, which comprises a “sorbed” fraction (potentially “desorbable” in the physicochemical conditions encountered in the study estuaries) and a “non-exchangeable” fraction (Cd incorporated in the crystalline matrix, co-precipitated in various mineral phases, etc.).

Typical Cd behavior in macrotidal estuaries was well reproduced using average and maximum sorption properties (Figs. 12 and 13), and featured the classic bell-shaped CD D curve. Maximum dissolved Cd concentrations remained similar notwithstanding particle type or the position of the turbidity maximum: approximately 80 ng L^{-1} using average properties, with greater variations ($30\text{--}50 \text{ ng L}^{-1}$) according to particle type using maximum properties. Using minimum properties (Fig. 14), maximum dissolved Cd concentrations were restricted to very low salinity zones.

In all cases, maximum dissolved Cd migrated towards higher salinities at the turbidity peak.

6.3

Simulation of the Presence of a Second Turbidity Maximum

This scenario aimed to evaluate the impact of a second turbidity maximum in more saline waters. This situation, which stems from hydrodynamic factors, can be encountered in macrotidal estuaries such as the Loire and Gironde.

Using average properties (Fig. 15), particle types only differed significantly with zero salinity. The highest turbidity peak was clearly correlated with a minimum percentage of dissolved Cd. Adding a second turbidity maximum resulted in a slight sag in the Cd % curve.

Using minimum properties (Fig. 16), particle influence was only visible at the first peak; this was particularly true for Loire and Gironde particles, which have the highest GSC.

The impact of two turbidity maxima is major in the maximum sorption property scenario (Fig. 17). Dissolved Cd percentages remain low until salinity reaches about 10, in particular for Loire and Seine particles which have high GSC.

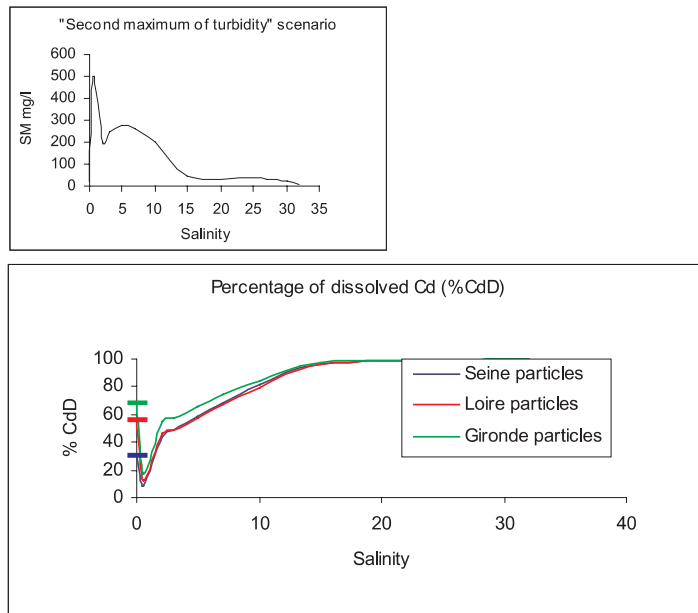


Fig. 15 "Second maximum of turbidity" scenario. Mean sorption properties simulation

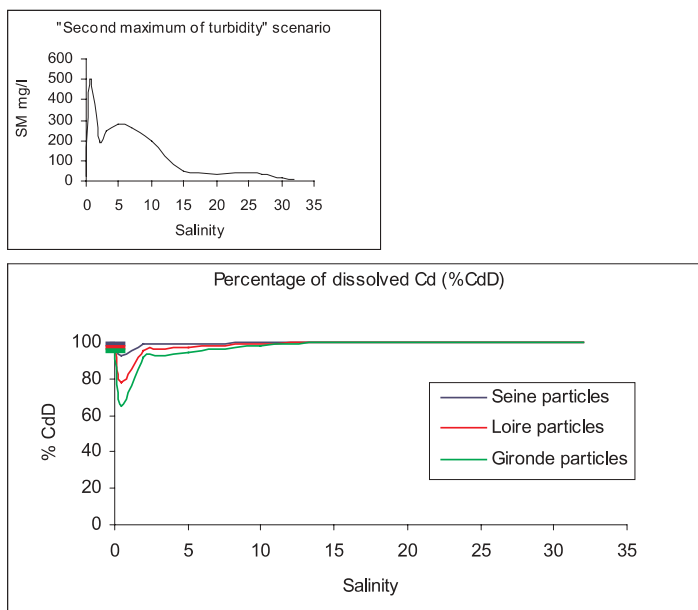


Fig. 16 "Second maximum of turbidity" scenario. Minimum sorption properties simulation

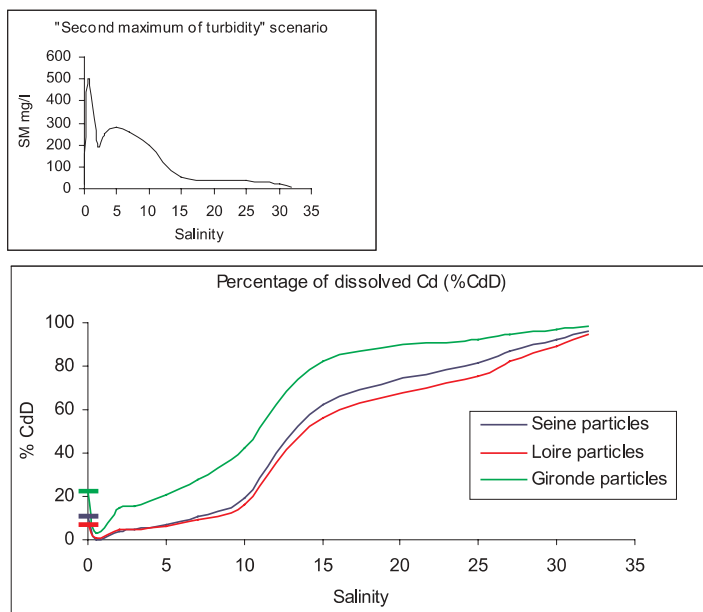


Fig. 17 “Second maximum of turbidity” scenario. Maximum sorption properties simulation

6.4

Simulation of Turbidity Peaks

The presence of major turbidity peaks, in any salinity range, is often encountered when mud deposit zones are eroded.

Using average and maximum sorption properties, turbidity peaks were shown to have a high impact, even in highly saline waters (Figs. 18 and 20). Differences in particle types were far more marked when maximum properties were used. The impact of turbidity peaks on particles with low GSC was minimal (Fig. 19), especially with high salinity. In this case, Cd behavior proved to be quasi-conservative.

7

Summary and Conclusions

We selected Cd to explore the impact of particle surface properties on the fate and speciation of contaminants in macrotidal estuaries due to its high reactivity. The behavior of Cd – which is highly sensitive to dissolved/particulate exchanges – was simulated using sorption properties representative of particles from different estuaries to demonstrate that:

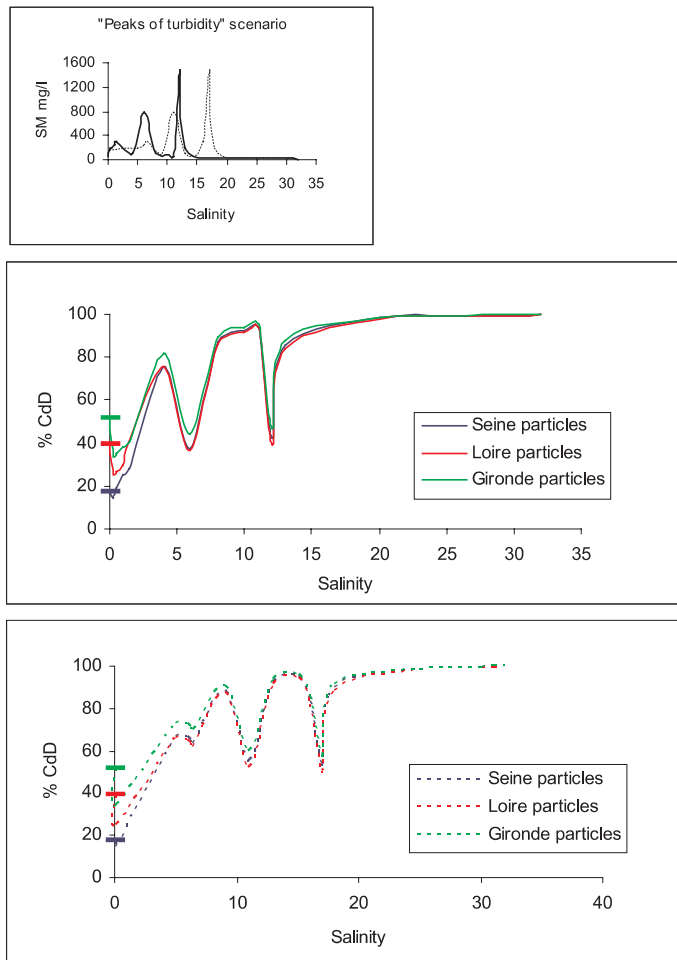


Fig. 18 Percentage of dissolved Cd (%CdD): "Peaks of turbidity" scenario. Mean sorption properties simulation

- Even in the case of weak sorption properties and virtually conservative Cd behavior within the estuary, major differences according to particle origin can be observed when SM concentrations are high and salinity is close to zero (Fig. 10), especially if GSC are significantly different (around factor 7) (Fig. 8).
- Using average properties (representing the overall measurements conducted on various samples), simulation of the dissolved/particulate partition gives comparable results notwithstanding particle origin, due to the fact that GSC is relatively similar (Fig. 8). The scenarios simulated as a whole highlighted the instrumental role of particles in all salinity ranges.

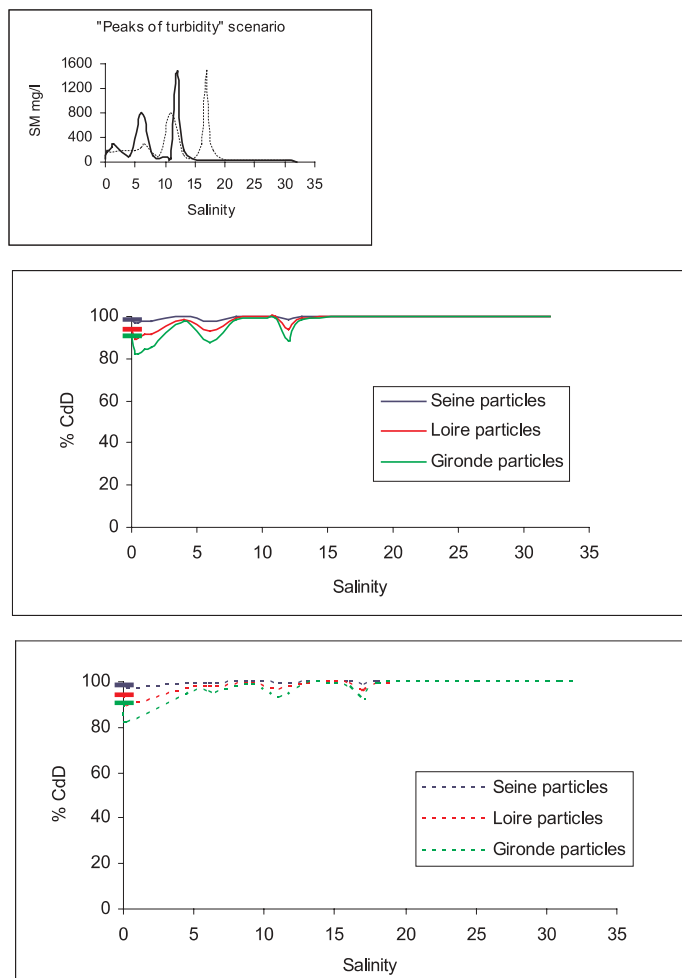


Fig. 19 Percentage of dissolved Cd (%CdD): "Peaks of turbidity" scenario. Minimum sorption properties simulation

- When sorption capacity is high, variations in particles have a far greater impact on Cd behavior, even in high salinity ranges.

The evaluation of GSC highlighted the relative uselessness of standard characteristics (POC, Al, Fe, Mn, SA, etc.) employed to ascertain particle sorption capacity to contaminants. More explicit parameters, i.e., nature and density of surface sites, acidity intrinsic properties and complexation constants, and their natural variabilities, are necessary to efficiently evaluate particle reactivity with regards to a given element in various physicochemical conditions.

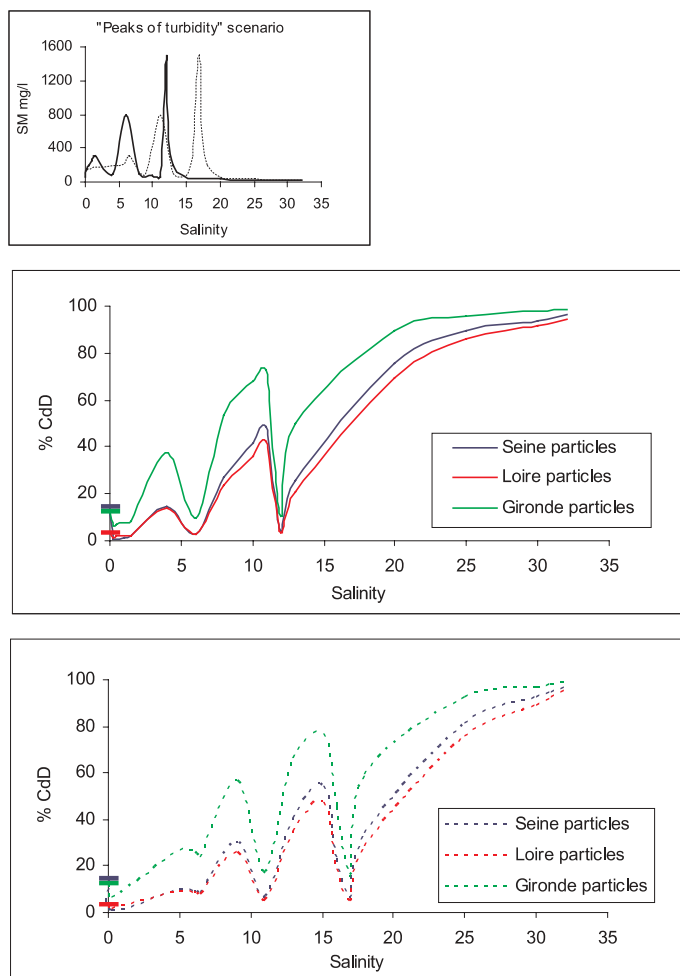


Fig. 20 Percentage of dissolved Cd (%CdD): "Peaks of turbidity" scenario. Maximum sorption properties simulation

The comparison of Cd measurements (Table 4) showed average Cd concentrations in suspended matter in both the upstream and mixing zones to be significantly higher in the Seine estuary than in the other study estuaries (Loire and Gironde). One of the reasons put forward for this could be the higher sorption capacity of Seine particles (as per the estimated K_m value). If we consider the average GSC of particles taken from the various estuaries (Fig. 8), it is interesting to note that Seine particles only have significantly higher sorption capacities than particles from the other two study estuaries when salinity is close to zero. When salinity exceeds 5, the average reactivity of Seine particles decreases strongly, to around that of Gironde particles. The

variations we observed in Seine particle sorption capacity versus water salinity could partially explain the differences in particulate Cd concentrations measured in the upstream and downstream zones.

The impact of particle surface properties is maximized when salinity is around zero and SM concentrations are high. The importance of the particulate phase is relative when salinity increases, due to the key role of chlorides in Cd speciation. This suggests that particle sorption properties have a major impact on the speciation of Cd-type elements, whose behavior is controlled by competition between the particulate phase and a major ligand associated with the dissolved phase (e.g., the ion chloride in the case of Cd). Hence, in macrotidal estuaries, space-time variations in terms of salinity gradient and SM quantity and type will contribute to dissolved/particulate partition and to contaminant fluxes to the ocean/continent interface.

From a modeling viewpoint, the results obtained suggest that it is possible to simulate (and forecast) the behavior of contaminants such as Cd in complex environments by evaluating various parameters experimentally. These parameters are used to characterize processes (surface complexation constant and acidity constants of surface sites) and particles (density of surface sites). Their value must be determined with sufficient accuracy, and their variability within the environment must be known.

Our study exclusively related to the role of particles in processes close to equilibrium, and did not take into account the dynamic aspect of processes, in particular the temporal evolution of turbidity and salinity gradients, which is of major importance in macrotidal estuaries. "Slow" processes, driven by particles, may also regulate the dynamics and speciation of trace metals in the estuarine environment, e.g., desorption and processes related to the mineralization of certain mineral phases (Fe and Mn oxides and organic matter), in particular in fine matter deposit zones and maximum turbidity zones.

Our results nevertheless showed that particle surface properties, evaluated on the basis of various parameters, are instrumental in non-conservative contaminant speciation in the estuarine environment. Their analysis enables us to understand and simulate, to a large extent, the fate of non-conservative contaminants whose behavior is controlled by competition between sorption and desorption processes.

References

1. Pritchard DW (1955) *Proc Am Soc Civ Engin* 8:1
2. Pritchard DW (1967) In: Lauff GH (ed) *Estuaries*. Washington American Association for Advancement of Science 83:158
3. Officer CB (1976) *Physical oceanography of estuaries (and associated coastal waters)*. Wiley, New York
4. Guézennec L, Romana LA, Goujon R, Meyer R (1999) *Seine-Aval: un estuaire et ses problèmes*, Programme Scientifique "Seine Aval", Fascicule no 1. IFREMER, Plouzané (France)

5. Stumm W, Morgan JJ (1981) *Aquatic chemistry*, 2nd edn. Wiley, New York
6. Uncles RJ, Stephens JA, Smith RE (2002) *Cont Shelf Res* 22:1835
7. Turner A, Millward GE (2002) *Coast Shelf Sci* 55:857
8. Turner A (1996) *Mar Chem* 54:27
9. Boyle EA, Edmond JM, Sholkovitz JR (1982) *Geochim Cosmochim Acta* 41:1313
10. Elbaz-Poulichet F, Huang WW, Martin JM, Zhu JX (1987) *Mar Chem* 22:125
11. Boutier B, Jouanneau JM, Chiffoleau JF, Latouche C, Phillips I (1989) La contamination de la Gironde par le cadmium, *Rapports Scientifiques et Techniques de l'IFREMER*. IFREMER, Plouzané (France)
12. Boutier B, Chiffoleau JF, Auger D, Truquet I (1993) *Coast Mar Sci* 36:133
13. Chiffoleau JF, Cossa D, Auger D, Truquet I (1994) *Mar Chem* 47:145
14. Krapiel AML, Chiffoleau JF, Martin JM, Morel FMM (1997) *Geochim Cosmochim Acta* 61:1421
15. Thouvenin B, Gonzalez JL, Boutier B (1997) *Mar Chem* 58:147
16. Chiffoleau JF, Auger D, Chartier E, Michel P, Truquet I, Ficht A, Gonzalez JL, Romana LA (2001a) *Estuaries* 24:1029
17. Chiffoleau JF, Claisse D, Cossa D, Ficht A, Gonzalez JL, Guyot T, Michel P, Miramand P, Oger C, Petit F (2001b) La contamination métallique, Programme scientifique "Seine Aval", Fascicule no 8. IFREMER Plouzané (France)
18. Comans RNJ, Van Dijk CPJ (1988) *Nature* 336:151
19. Elbaz-Poulichet F, Garnier JM, Guang DM, Martin JM, Thomas AJ (1996) *Coast Shelf Sci* 42:289
20. Guieu C, Huang WW, Martin JM, Yong Y (1996) *Mar Chem* 53:255
21. Guieu C, Martin JM (2002) *Estuar Coast Shelf Sci* 54:501
22. Garnier JM, Guieu C (2003) *Mar Environ Res* 55:5
23. Glangeaud L (1938) *Bulletin de la Société de Géologie de France* 8:599
24. Gallenne B (1974) Thèse de doctorat de 3^{ème} cycle, Université de Nantes
25. Phillips I (1980) Thèse de doctorat de 3^{ème} cycle, Université de Bordeaux I
26. Avoine J (1981) Thèse de doctorat de 3^{ème} cycle, Université de Caen
27. Jouanneau JM (1982) Thèse de doctorat d'état, Université de Bordeaux I
28. El Sayed M (1988) Thèse de doctorat d'état, Université de Bretagne Occidentale
29. Le Hir P, Ficht A, Silva Jacinto R, Lesueur P, Dupont JP, Lafite R, Brenon I, Thouvenin B, Cugier P (2001) *Estuaries* 24:950
30. Dange C (2002) Thèse de doctorat, Université de Reims Champagne-Ardenne
31. Boutier B, Chiffoleau JF, Gonzalez JL, Lazure P (1996) 5^{ème} Colloque International d'Océanographie du Golfe de Gascogne, La Rochelle, France
32. Boutier B, Chiffoleau JF, Gonzalez JL, Lazure P, Auger D, Truquet I (2000) *Oceanologica Acta* 23:745
33. Allen GP (1971) *CR Acad Sc* 273:2429
34. Gonzalez JL, Thouvenin B, Dange C, Fiandrino A, Chiffoleau JF (2001b) *Estuaries* 24:1041
35. Sposito G (1984) *The surface chemistry of soils*. Oxford University Press, New York
36. Garnier JM, Martin JM, Mouchel JM, Thomas AJ (1993) *Estuar Coast Shelf Sci* 36:315
37. Westall JC (1982) FITEQL. A computer program for determination of chemical equilibrium constants from experimental data. Technical Report 82-01. Department of Chemistry, Oregon State University, Corvallis
38. Gulmini M, Zelano V, Daniele PG, Prenesti E, Ostacoli G (1996) *Anal Chim Acta* 329:33
39. Wang F, Chen J, Forsling W (1997) *Water Res* 7:796
40. Muller B, Duffek A (2001) *Aquat Geochem* 7:107

41. Cossa D, Meybeck M, Idlafkih Z, Bombled B (1994) Etude pilote des apports en contaminants par la Seine. IFREMER Report DEL 94-13
42. Gonzalez JL, Thouvenin B, Chiffolleau JF, Miramand P (1999) Le cadmium: comportement d'un contaminant métallique en estuaire. Programme scientifique "Seine Aval", Fascicule no 10. IFREMER, Plouzané (France)
43. Bruland KW, Franks RP (1983) In: Wong CS, Boyle EA, Bruland KW, Burton JD, Goldberg ED (eds) Trace metals in sea water. NATO Conference Series IV, Mar Sci 9:395
44. Cossa D, Lassus P (1989) Le cadmium en milieu marin Biogéochimie et ecotoxicologie. IFREMER Report 16
45. Gonzalez JL, Boutier B, Chiffolleau JF, Auger D, Noel J, Truquet I (1991b) *Oceanol Acta* 6:559
46. Valenta P, Duursma EK, Merks AG, Ruetzel H, Nuernberg HW (1986) *Sci Total Environ* 53:41
47. Klinkhammer G, Bender ML (1981) *Estuar Coast Shelf Sci* 12:629
48. Gobeil C, Silverberg N, Sundby B, Cossa D (1987) *Geochim Cosmochim Acta* 51:589
49. Westerlund SFG, Anderson LG, Hall POJ, Iverfeldt A, Van Der Loeff RMM, Sundby B (1986) *Geochim Cosmochim Acta* 50:1289
50. Klinkhammer G, Heggie DT, Graham DW (1982) *Earth Planet Sci Lett* 61:211
51. McCorkle DC, Klinkhammer GP (1991) *Geochim Cosmochim Acta* 55:161
52. Gonzalez JL (1994) Evaluation des flux de contaminants à l'interface eau-sédiments en zone littorale *Oceanis* 3:23
53. Gonzalez JL, Boutier B, Auger D, Chartier E (2004) Les vasières intertidales et subtidales sont elles des sources de contaminants métalliques? In: Contribution à l'étude de la dynamique et de la spéciation des contaminants. Programme Scientifique Seine-Aval Report
54. Shiller AM, Boyle EA (1991) *Geochim Cosmochim Acta* 11:3241
55. Cossa D (1990) Chemical contaminants in the St. Lawrence estuary and Saguenay Fjord. In: El-Sabh MI, Silverberg N (eds) *Oceanography of a large-scale estuarine system: The St. Lawrence*. Springer, Berlin Heidelberg New York, p 239
56. Baeyens W, Decadt G, Dedeurwaerder H, Dehairs F, Gillain G (1984) Symposium on contaminant fluxes through the coastal zone, Nantes, France
57. Guieu C, Martin JM, Thomas AJ, Elbaz-Poulichet F (1991) *Mar Poll Bull* 22:176
58. Thomas AJ, Huang WW (1996) Les métaux traces particulaires et dissous (Cd, Cu, Ni, Pb et Zn) dans le Rhône à Arles durant le cycle annuel juin 1994-mai 1995: origines, concentrations et flux. Agence de l'Eau Rhône-Méditerranée-Corse Report
59. Gonzalez JL, Dange C, Thouvenin B (2001a) *Hydroécologie Appliquée* 1:37
60. Laurier FJG, Cossa D, Gonzalez JL, Breviere E, Sarazin G (2003) *Geochim Cosmochim Acta* 18:3329
61. Stumm W, Kummer R, Sigg L (1980) *Croat Chem Acta* 53:291
62. Davis JA, Kent DB (1990) Surface complexation modelling in aqueous geochemistry. In: Hochella MF, White AF (eds) *Mineral-water interface geochemistry, reviews in mineralogy*. Mineralogical Society of America, Washington, p 177
63. Dzombak DA, Morel FMM (1987) *J Hydraul Eng* 113:430
64. Dzombak DA, Morel FMM (1990) *Surface complexation modeling: Hydrous ferric oxide*. Wiley, New York
65. Van der Weidjen CH, Arnoldus MJHL, Meurs CJ (1977) *Neth J Sea Res* 11:130